

A New Self-organizing Interval Type-2 Fuzzy Neural Network for Multi-Step Time Series Prediction

Fulong Yao*, Wanqing Zhao, *Member, IEEE*, Matthew Forshaw, Yang Song, *Member, IEEE*

Abstract—This paper proposes a new self-organizing interval type-2 fuzzy neural network with multiple outputs (SOIT2FNN-MO) for multi-step time series prediction. Differing from the traditional six-layer IT2FNN, a nine-layer network is developed to improve prediction accuracy, uncertainty handling and model interpretability. First, a new co-antecedent layer and a modified consequent layer are devised to improve the interpretability of the fuzzy model for multi-step predictions. Second, a new transformation layer is designed to address the potential issues in the vanished rule firing strength caused by high-dimensional inputs. Third, a new link layer is proposed to build temporal connections between multi-step predictions. Furthermore, a two-stage self-organizing mechanism is developed to automatically generate the fuzzy rules, in which the first stage is used to create the rule base from empty and perform the initial optimization, while the second stage is to fine-tune all network parameters. Finally, various simulations are carried out on chaotic and microgrid time series prediction problems, demonstrating the superiority of our approach in terms of prediction accuracy, uncertainty handling and model interpretability.

Index Terms—Interval type-2 fuzzy neural network (IT2FNN), Uncertainty handling, Multi-step time series prediction, Interpretability

I. INTRODUCTION

TIME series data, a sequence of observations recorded at constant time intervals, is prevalent in various fields such as engineering [1], [2], economics [3], [4], meteorology [5] and health [6]. These data often exhibit temporal dependencies and trends, making them valuable for understanding and forecasting future system behaviours. However, time series observations in reality are always inherent to data uncertainties, such as stemming from noises in sensor measurements, disturbances in system operations and even errors in simulation and predictive models [7], [8]. Such uncertainties can propagate dramatically in the downstream modelling and decision-making processes. This brings fundamental challenges to time series prediction problems. Traditional machine learning methods, such as support vector machines (SVM) [9], long short-term memory (LSTM) [10] and convolutional neural network-LSTM (CNN-LSTM) [11], are often limited in capturing the diverse sources of uncertainty. This has led to suboptimal predictive performance and unreliable predictions [12], especially when further incorporated for decision making purposes.

Fulong Yao, Wanqing Zhao and Matthew Forshaw are with the School of Computing, Newcastle University, Newcastle upon Tyne, NE4 5TG, UK. Yang Song is with the School of Mechanical and Electrical Engineering and Automation, Shanghai University, Shanghai, 200444, China. Corresponding author: Fulong Yao (F.Yao3@newcastle.ac.uk)

In the past several decades, the fuzzy logic system (FLS) has been a great success in time series prediction, owing to the ability to handle linguistic and numerical uncertainties [13]. For example, Pourabdollah et al. [14] proposed a dynamic FLS based on a novel non-singleton fuzzification to improve the prediction accuracy of noisy time series (e.g., Mackey-Glass and Lorenz time series). Jafri et al. [15] developed a novel fuzzy logic for hourly wind prediction and achieved remarkable performance. However, FLS suffers from its root in handcrafted fuzzy rules and prior knowledge about the system, as well as potential challenges in generalizing to new data [16]. To address these limitations, researchers have explored a range of fuzzy neural networks (FNNs), combining the learning ability of artificial neural networks with the interpretability of fuzzy logic. Among these, adaptive-network-based fuzzy inference system (ANFIS) [17] has gained the widest recognition. It allows to learn complex patterns from data, while incorporating fuzzy logic for semi-transparent reasoning. Given this, a number of ANFIS-based time series models have been developed. For instance, Melin et al. [18] designed an ensemble of ANFIS to minimize the prediction error of the Mackey–Glass time series and Mexican stock exchange. Inyurt and Razin [19] employed ANFIS to solve a complex ionosphere prediction problem and achieved good accuracy and resilience to noise.

However, the aforementioned models are designed based on type-1 fuzzy sets (with a crisp membership grade). Once the type-1 membership functions (MF) are determined, all uncertainties disappear [8], [20]. This makes it difficult for type-1 FNN (T1FNN) to directly handle the uncertainties in data. To remedy this issue, type-2 FNNs (T2FNNs) was developed using type-2 fuzzy sets (T2FS), which increases fuzziness in expression by designing a three dimensional fuzzy membership function. The increased fuzziness can enhance the ability to handle inaccurate information with the same number of rules [21]. Therefore, it becomes particularly effective when data is too uncertain to give the exact membership grades of a fuzzy set (FS) [22]. However, general T2FNN often requires extensive computation in type-reduction as part of the defuzzification process, which limits its real-world applications. This has led to the development of multiple variants of T2FNN. Among these, interval type-2 fuzzy neural networks (IT2FNNs), which are based on interval type-2 fuzzy sets (IT2FS), have become increasingly prominent and widely recognized.

Recently, a number of IT2FNN approaches have been developed with a Takagi-Sugeno-Kang (TSK) consequent for handling data uncertainty and improving model accuracy. For example, Salimi-Badr [23] proposed an interval type-

2 correlation-aware fuzzy neural network (IT2CAFNN) for nonlinear dynamic system modeling problems (e.g., time-series predictions and system identification). To address the uncertainty, a shapeable IT2FS was designed to adaptively build the shape of fuzzy membership functions. Ashfahani et al. [24] developed an evolving type-2 quantum-based fuzzy neural network (eT2QFNN) for radio frequency identification (RFID) localization in a Manufacturing Shopfloor, in which an interval type-2 quantum fuzzy set with uncertain jump positions was designed to address noises in data. Apart from improving the antecedent by using IT2FS, some studies were also conducted on enhancing the rule consequent. Beke and Kumbasar [25] designed a composite learning framework for interval type-2 fuzzy neural network (CLF-IT2NN), where a total of 12 CLF-IT2FNN approaches were summarized based on combinations of different types of rule antecedents and consequents.

Moreover, some researchers have tried to improve the performance of IT2FNN by modifying the network structure. For instance, Luo and Wang [26] proposed an interval type-2 LSTM fuzzy neural network (IT2FNN-LSTM) to improve the accuracy and uncertainty quantification for long-term time series predictions. More related works can be found in [8], [27]. It is worth noting that all these IT2FNN models are consisted of the traditional six-layer network, i.e., input layer, antecedent layer, rule layer, consequent layer, type reduction layer and output layer. However, as the input size increases, such 6-layer networks may suffer from vanished rule firing strength. Specifically, in the IT2FNN model, firing strength is computed by multiplying all fuzzy membership grades associated with the inputs together. Thus, the increase in the number of model inputs will result in a decrease in the rule firing strength (due to fuzzy membership grade being between 0 and 1). When the input dimension is too large, all rules will fail to be fired for an effective model output, causing training to collapse. More discussion will be provided in Section II.

On the other hand, due to the limited predictive insights offered by a single-step prediction in practical applications, it is often required to perform multi-step ahead predictions into the future. At present, this can be done with three popular schemes: sliding window (SW), paralleling model (PM) and multiple outputs (MO). Many related works have been summarized in [28], [29], [30]. Generally, the SW scheme involves training a single-output model and then successively using this model to generate multiple predictions based on previously predicted values. However, this scheme relies on previously predicted values, which can accumulate prediction errors over time. In contrast, the PM scheme involves training multiple single-output models, each making a prediction for a different future time step. This obviously requires training and managing multiple predictive models, resulting in increased computational and storage requirements. Moreover, the single-step forecasting may hinder the model from capturing long-term dependencies in time series [8]. As a result, this paper will investigate the MO scheme, where a multi-output model will be built, with each output giving a future prediction. Although there have been some studies on IT2FNN for multi-step time series

prediction using MO scheme (e.g., [31] and [32]), they all ignored the temporal connections between multiple outputs, which can lead to unnecessary uncertainties in prediction. Unlike the traditional multi-output modeling (e.g., multi-variant prediction), a continuous temporal relationship is also expected between multiple time series predictions.

Moreover, although IT2FNN provides good interpretability in the single-output prediction through the design of IF-THEN rules, this interpretability can decrease significantly in the case of MO-based multi-step ahead predictions as each rule is required to account for a mixture of multiple predictions. Furthermore, IT2FNN can identify complex nonlinear system behaviours but at the expense of using a large number of fuzzy rules, which can lead to rule explosion [33]. Self-organizing IT2FNN with advanced rule learning capabilities has recently attracted widespread attention and proved promising in solving the rule explosion, as described in [34], [35], [36], [37]. However, current research in this field mainly focuses on single-step ahead predictions, with limited studies addressing multi-step predictions (particularly those involving MO-based models).

To address the above challenges, this paper proposes a novel self-organizing interval type-2 fuzzy neural network based on the MO scheme (SOIT2FNN-MO) for multi-step time series predictions. The main contributions can be summarized as: 1) a new link layer is proposed to enhance temporal connections between multi-step predictions; 2) a new co-antecedent layer and a modified consequent layer are designed to improve the interpretability of fuzzy network; 3) a new transformation layer is devised to address the potential issues in the vanished rule firing strength caused by high-dimensional inputs; 4) a two-stage self-organizing mechanism is developed to automatically generate the fuzzy rules, in which the first stage focuses on forming the rule base and performing initial optimization and the second stage is to fine-tune all model parameters together.

The rest of this paper is structured as follows. Section II and Section III present the network structure and learning mechanism of the proposed SOIT2FNN-MO, respectively. Section IV provides a detailed performance evaluation, while Section V concludes the paper.

II. SOIT2FNN-MO STRUCTURE

This section introduces an interval type-2 fuzzy neural network with multiple outputs (SOIT2FNN-MO) for multi-step time-series prediction problems. Fig. 1 shows the overall structure of the SOIT2FNN-MO. Differing from the traditional six-layer IT2FNN [38], [39], [40], a nine-layer network is devised here by introducing three additional layers (4, 5, 9) to improve the prediction accuracy and model interpretability, accounting for the nature of multi-step ahead predictions. In detail, we design a new co-antecedent layer (Layer 4) to improve the interpretability of the rule antecedent for multiple outputs, a new transformation layer (Layer 5) to address the potential issues in the vanished rule firing strength, and a link layer (Layer 9) to enhance sequential connections among multiple predictions. In addition, we have also made some modifications to layer 6 (consequent layer) to enhance the interpretability of the rule consequent

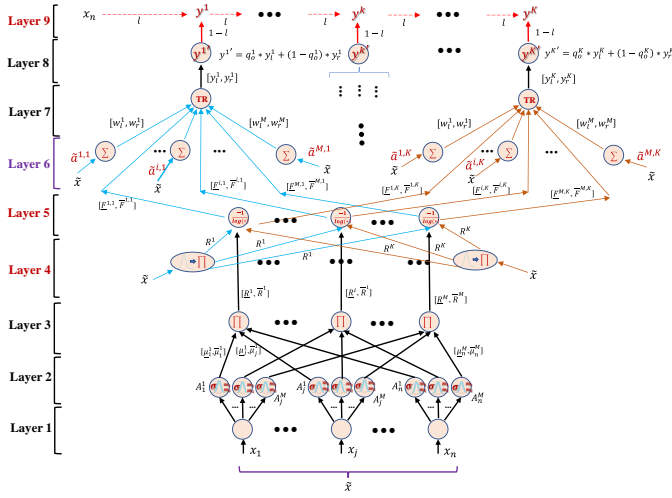


Fig. 1: Structure of the proposed SOIT2FNN-MO

for predictions at different steps ahead. Each layer and its function are now detailed as follows:

Layer 1 (Input Layer): The time-series input is given by $\tilde{x} = \{x_1, x_2, \dots, x_j, \dots, x_n\}$, where n is the total number of model inputs including scenarios of either univariate or multivariate inputs. For example, to predict from the past three values of 2 variables (p_1 and p_2), \tilde{x} would be $\{p_1(t-2), p_1(t-1), p_1(t), p_2(t-2), p_2(t-1), p_2(t)\}$. Each node in layer one represents a crisp input without any mathematical transformations.

Layer 2 (Antecedent Layer): This layer is also referred to as the fuzzification layer. Here, each node employs a Gaussian interval type-2 membership function (IT2MF) to perform a fuzzification operation that converts crisp inputs into interval fuzzy values. In this paper, we adopt a Gaussian MF with a fixed standard deviation but an uncertain mean value (see Fig. S1 in the supplementary materials):

$$\begin{aligned} \mu_{\tilde{A}_j^i} &= \exp\left\{-\frac{1}{2}\left(\frac{x_j - m_{1,j}^i}{\sigma_j^i}\right)^2\right\} \\ &= N(m_{1,j}^i, \sigma_j^i; x_j), m_{1,j}^i \in [m_{1,j}^i, m_{2,j}^i] \end{aligned} \quad (1)$$

where \tilde{A}_j^i is the IT2FS for the j -th input with regard to the i -th rule. Each Gaussian IT2MF can be further represented by an upper membership function (UMF) and a lower membership function (LMF) as follows:

$$\overline{\mu}_j^i(x_j) = \begin{cases} N(m_{1,j}^i, \sigma_j^i; x_j), & \text{if } x_j < m_{1,j}^i; \\ 1, & \text{if } m_{1,j}^i \leq x_j \leq m_{2,j}^i; \\ N(m_{2,j}^i, \sigma_j^i; x_j), & \text{if } x_j > m_{2,j}^i. \end{cases} \quad (2)$$

$$\underline{\mu}_j^i(x_j) = \begin{cases} N(m_{2,j}^i, \sigma_j^i; x_j), & \text{if } x_j \leq \frac{m_{1,j}^i + m_{2,j}^i}{2}; \\ N(m_{1,j}^i, \sigma_j^i; x_j), & \text{if } x_j > \frac{m_{1,j}^i + m_{2,j}^i}{2}. \end{cases} \quad (3)$$

where σ_j^i is the standard deviation of both LMF and UMF, and $m_{1,j}^i$ and $m_{2,j}^i$ are the means of LMF and UMF, respectively. Thus, the output of layer two is an interval $[\underline{\mu}_j^i(x_j), \overline{\mu}_j^i(x_j)]$. To ensure $\overline{\mu}_j^i(x_j) \geq \underline{\mu}_j^i(x_j)$ by the definition of IT2FS, the constraint $m_{1,j}^i \leq m_{2,j}^i$ should always be met.

Here, data uncertainty is handled by using the Gaussian IT2FS, which represents an interval of membership values $[\underline{\mu}_j^i(x_j), \overline{\mu}_j^i(x_j)]$ rather than crisp points [37]. This enhances robustness and accuracy in prediction tasks when data is noisy or imprecise.

Layer 3 (Rule Layer): This layer is also referred to as the firing strength of rules. This layer contains information regarding the influence range of each rule (there are M rules in total, as shown in Fig. 1). Here, each node represents a fuzzy rule, and its output gives the lower (\underline{R}^i) and upper (\overline{R}^i) firing strength of this rule. Mathematically, the two firing strengths are computed by performing a fuzzy meet operation using the following algebraic product:

$$\underline{R}^i = \prod_{j=1}^n \underline{\mu}_j^i(x_j); \quad \overline{R}^i = \prod_{j=1}^n \overline{\mu}_j^i(x_j) \quad (4)$$

Layer 4 (Co-antecedent Layer): This layer is introduced to further improve the interpretability of the rule antecedent. There are K nodes in this layer, each one corresponding to a specific time-series prediction (from 1-step ahead to K -step ahead). Within each node, two operations are performed, i.e., Gaussianization and algebraic product (5):

$$\mu_j^k(x_j) = N(m_j^k, \sigma_j^k; x_j); \quad R^k = \prod_{j=1}^n \mu_j^k(x_j) \quad (5)$$

Remark 1: Although both the second and fourth layers incorporate Gaussian MFs, they differ in nature. The second layer employs the Gaussian IT2MF with an interval output, while the fourth layer adopts a normal Gaussian MF with a crisp output.

Remark 2: The second and fourth layers serve distinct purposes. The second layer functions as a shared layer across all model outputs (each IT2MF simultaneously affects all outputs), representing the commonalities across multiple model outputs. On the other hand, the fourth layer will only influence an individual model output, i.e. the prediction at a specific time step. By considering both the commonalities and individualities in the rule antecedent, the interpretability of the IT2FNN for time series predictions can thus be enhanced.

Layer 5 (Transformation Layer): This layer is devised to address the potential issue of vanished rule firing strength that occurs in the case of high-dimensional inputs. Generally, in MO-based time series prediction, as the number of outputs increases, it is advisable to expand the input dimension to get more historical patterns and features [41]. However, as the Gaussian membership grade is constrained to the range $[0,1]$, increased number of model inputs can lead to a rapid decrease in the firing strength (see (4),(5)). In the practice of optimization processes, when $n \geq 9$, the product of $\underline{R}^i R^k$ and $\overline{R}^i R^k$ can be lower than $1e-35$. This causes numerical instability and the problem of vanished rule firing strength (with values such as ‘inf’ or ‘-inf’).

Here, by leveraging the properties of logarithmic operations, we devise a novel aggregation function to merge the shared firing strength interval $[\underline{R}^i, \overline{R}^i]$ with the individualized firing strength R^k . This aggregation function employs

the $\log(\cdot)$ to convert the product operation into a sum operation, effectively solving the vanished rule firing strength problem. Each node in this layer represents an aggregation function, producing an aggregated firing strength interval $F^{i,k}$ as the output. The expression for the aggregation function is expressed as:

$$F^{i,k} = [\underline{f}^{i,k}, \bar{f}^{i,k}], \quad i = 1, \dots, M; \quad k = 1, \dots, K \quad (6)$$

where K is the number of model outputs (i.e., the number of steps to be predicted), and $\underline{f}^{i,k}$ and $\bar{f}^{i,k}$ are defined as:

$$\underline{f}^{i,k} = -\frac{1}{\log(\underline{R}^i R^k)} = -\frac{1}{\sum_{j=1}^n \log(\underline{\mu}_j^i(x_j) \mu_j^k(x_j))} \quad (7)$$

$$= -\frac{1}{\sum_{j=1}^n \log(\underline{\mu}_j^i(x_j)) + \sum_{j=1}^n \log(\mu_j^k(x_j))}$$

$$\bar{f}^{i,k} = -\frac{1}{\log(\bar{R}^i R^k)} = -\frac{1}{\sum_{j=1}^n \log(\bar{\mu}_j^i(x_j) \mu_j^k(x_j))} \quad (8)$$

$$= -\frac{1}{\sum_{j=1}^n \log(\bar{\mu}_j^i(x_j)) + \sum_{j=1}^n \log(\mu_j^k(x_j))}$$

Remark 3: In practice, ‘when $n \geq 9$, the product of $\underline{R}^i R^k$ and $\bar{R}^i R^k$ can be lower than $1e-35$.’ This is drawn from IT2FNN-based prediction models for microgrid electricity prices; more details regarding this simulation will be provided in Section IV-B.

Remark 4: If the membership grades (e.g. \underline{R}^i , \bar{R}^i and R^k) lie in $[0.0001, 1]$, the values of $\log(x)$ will fall within the range of $[-9.2103, 0]$. Thus, the computation of F is entirely manageable, thereby avoiding the issue of vanished rule firing strength. In fact, as long as the initial parameters of Gaussian MFs are appropriately chosen, occurrences of membership grades smaller than 0.001 are less likely.

Remark 5: \underline{R}^i or \bar{R}^i is associated with a specific rule and is independent of any output, whilst R^k is exclusively linked to a particular output and is unrelated to any rule. As a result, the interval output $[\underline{f}^{i,k}, \bar{f}^{i,k}]$ is both rule-dependent and output-related.

Layer 6 (Consequent Layer): Each node in this layer represents a TSK rule consequent, operating as a linear combination of the model inputs \tilde{x} . Unlike traditional IT2FNN, where one rule (in layer 3) corresponds to just one TSK node, here each rule corresponds to K nodes. Therefore, there are a total of $K * M$ nodes in this layer. The output of this layer can be represented as the following interval set $[w_l^{i,k}, w_r^{i,k}]$ in (9). In this way, the prediction at each step has a specific rule consequent, thus improving the interpretability of the consequent part of IT2FNN. Additionally, the interval set of this layer further enhances the uncertainty handling and reliability of the prediction network [25].

$$[w_l^{i,k}, w_r^{i,k}] = [c_0^{i,k} - s_0^{i,k}, c_0^{i,k} + s_0^{i,k}] + \sum_{j=1}^n [c_j^{i,k} - s_j^{i,k}, c_j^{i,k} + s_j^{i,k}] x_j \quad (9)$$

The following equations can thus be derived:

$$w_l^{i,k} = \sum_{j=1}^n c_j^{i,k} x_j + c_0^{i,k} - \sum_{j=1}^n s_j^{i,k} |x_j| - s_0^{i,k} \quad (10)$$

$$w_r^{i,k} = \sum_{j=1}^n c_j^{i,k} x_j + c_0^{i,k} + \sum_{j=1}^n s_j^{i,k} |x_j| + s_0^{i,k} \quad (11)$$

where $x_0 \equiv 1$, $w_*^{i,k}$ is the k -th output of the i -th rule. For $\forall i$ and $\forall k$, the consequent part must satisfy $w_l^{i,k} \geq w_r^{i,k}$; thus $s_0^{i,k} \geq 0$ and $s_j^{i,k} \geq 0$ hold [25].

Layer 7 (Type Reduction Layer): This layer is responsible for converting type-2 into type-1 fuzzy sets. Each node in this layer corresponds to a linguistic output variable [42]. Instead of adopting traditional K-M iterative method [43], the output functions in (12) and (13) are used in this paper to perform the type reduction more efficiently. Here, the factors q_l^k and q_r^k are employed to adaptively adjust the lower and upper positions of the k -th interval output $[y_l^k, y_r^k]$.

$$y_l^k = \frac{(1 - q_l^k) \sum_{i=1}^M \underline{f}^{i,k} w_l^{i,k} + q_l^k \sum_{i=1}^M \bar{f}^{i,k} w_l^{i,k}}{\sum_{i=1}^M (\underline{f}^{i,k} + \bar{f}^{i,k})} \quad (12)$$

$$y_r^k = \frac{(1 - q_r^k) \sum_{i=1}^M \underline{f}^{i,k} w_r^{i,k} + q_r^k \sum_{i=1}^M \bar{f}^{i,k} w_r^{i,k}}{\sum_{i=1}^M (\underline{f}^{i,k} + \bar{f}^{i,k})} \quad (13)$$

Noted, we have $q_l^k \in [0, 1]$ and $q_r^k \in [0, 1]$ in the above equations.

Layer 8 (Defuzzification Layer): Each node in this layer gives a crisp output that corresponds to the prediction at a future time step. This can be computed by the following defuzzification equation:

$$y^{k'} = q_o^k y_l^k + (1 - q_o^k) y_r^k \quad (14)$$

where $q_o^k \in [0, 1]$ is the weight that balances the importance between y_l^k and y_r^k .

Layer 9 (Link Layer): In MO-based time series prediction, it usually assumes that the model outputs are independent of each other, which breaks the temporal connections between predictions at different time steps. To make the proposed SOIT2FNN-MO suitable for multi-step ahead predictions, we devise a new link layer here to build such a connection, as expressed in (15). This layer ensures that the predictions are not only determined by the model inputs, but also affected by predictions from its preceding steps. This will ultimately improve the prediction accuracy as well as its stability.

$$y^k = \begin{cases} (1 - l)y^{k'} + lx_n, & \text{if } k = 1; \\ (1 - l)y^{k'} + ly^{k-1}, & \text{if } k > 1. \end{cases} \quad (15)$$

Here, $l \in [0, 1]$ is the weight factor balancing the impact between the current and preceding predictions.

III. LEARNING METHOD

Given the proposed SOIT2FNN-MO, this section presents a two-stage self-organizing learning mechanism to determine both the model structure and parameters. The implementation steps are summarised in Algorithm 1. Here, the first stage is used to create the rule base from empty and perform initial parameter optimization, while the second stage is designed to fine-tune all model parameters together.

A. Pre-stage: Normalization and FCM

1) *Normalization*: To prevent the distribution of membership grades from becoming overly dispersed, normalizing the inputs is an important step. In this paper, the max-min scaling is simply employed to perform the normalization,

2) *Clustering*: Partitioning the input space into local regions with similar system behaviours through clustering can effectively enhance the adaptability of IT2FNN model to diverse data patterns [39], [44]. The derived clusters can be used to build the rule base with reduced computational complexity and improved model interpretability [45]. Given this, Fuzzy C-Means (FCM) [46] is employed in this paper to generate an initial number of N_c clusters, which will serve as the basis for structure learning of SOIT2FNN-MO. Here, the centroid and width of each cluster has the opportunity to be selected as antecedent parameters in layer 2, thus generating a potential fuzzy rule. Once a cluster is selected, antecedent parameters can be determined as:

$$m_{1,j}^i = m_j^c(1 - \Upsilon); \quad m_{2,j}^i = m_j^c(1 + \Upsilon); \quad \sigma_j^i = \sigma_j^c \quad (16)$$

where $\Upsilon = 0.1$ represents the uncertainty in the mean value (centroid) of the cluster, m_j^c and σ_j^c are the mean and STD of c -th cluster, respectively.

The initialization of co-antecedent parameters in layer 4 is much easier. Each co-antecedent MF corresponds to one output, and the quantity does not vary with the total number of rules. Given this, the initial co-antecedent parameters (e.g., m_j^k and σ_j^k) can be directly set to the mean and standard deviation of the set composed of all x_j , applicable to all co-antecedent MFs:

$$m_j^k = m_j^c; \quad \sigma_j^k = \sigma_j^c \quad (17)$$

where m_j^c and σ_j^c are the mean and standard deviation of the j -th input set.

B. Stage 1: Self-organizing Structure Learning

1) *Rule growing step*: The rule growing step is devised to generate rules in sequence (i.e., each episode can generate at most one rule) until a new rule no longer brings a significant improvement in the prediction accuracy. For each potential rule generation, the flowchart is shown in Fig. 2 and the implementations are depicted in Algorithm 2.

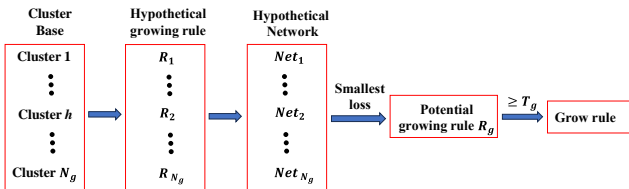


Fig. 2: Flowchart of the rule growing step

Specifically, each cluster obtained from FCM is used to make up a new hypothetical rule R_h . This hypothetical rule R_h , together with the existing rules, forms a hypothetical network Net_h . In this hypothetical network, the antecedent parameters (in Layer 2) are directly determined by the selected clusters as in (16). The remaining parameters (a

Algorithm 1: Learning Method of SOIT2FNN-MO

Input : \tilde{x}, \tilde{y}
Procedure:

- 1 Normalize \tilde{x} and initialize learning parameters and model weights;
- 2 Group \tilde{x} into N_c clusters using *FCM* and store them in a cluster base B^C ;
- 3 Define the rule number $N_r = 0$, status flag $F_s = 0$;
- 4 Create an empty rule base B^R and an empty base B^S to store generated rules and selected clusters later;
- 5 **for** $i = 1$ to $Episode_{max}$ **do**
- 6 ----- **Stage 1** -----
- 7 Jump to **Algorithm 2** for identifying the next potential rule to be added;
- 8 **if** $L_{hr} - L_g \geq T_g$ **then**
- 9 Add the new rule R_g into rule base B^R ;
- 10 Assign $L_{hr} = L_g$; $F_s = 1$;
- 11 Move C_g from B^C to B^S ;
- 12 Update parameters using Net_g ;
- 13 **else**
- 14 **if** $Size(B^R) \leq 1$ **then**
- 15 **if** $F_s == 3$ **then**
- 16 **break**;
- 17 **else**
- 18 $F_s = 3$;
- 19 **else**
- 20 Jump to **Algorithm 3** for identifying the least significant rule to be removed;
- 21 **if** $L_r - L_{hr} \geq T_r$ **then**
- 22 **if** $F_s == 3$ **then**
- 23 **break**;
- 24 **else**
- 25 $F_s = 3$;
- 26 **else**
- 27 Remove R_r from the rule base B^R ;
- 28 $L_{hr} = L_r$; $F_s = 2$;
- 29 Move C_r from B^S back to B^C ;
- 30 Update parameters using Net_r ;
- 31 ----- **Stage 2** -----
- 32 **if** $F_s == 3$ **then**
- 33 Jump to **Algorithm 4** for global optimization;
- 34 $L_{hr} = L_{gl}$, then update parameters using Net_{gl} ;

Output : Trained SOIT2FNN-MO

total number of $2 \cdot K \cdot n + (n+1) \cdot 2 \cdot M \cdot K + 2 \cdot K + K + 1$ in Layers 4,6,7,8,9) are optimized using stochastic gradient descent (SGD). In this way, N_h hypothetical rules will be generated here, but only the hypothetical rule corresponding to the network Net_h with the smallest loss L_g (defined as mean squared error) is qualified to become a potential growing rule R_g . Here, the mean squared error (MSE) of all training set is employed as the loss criterion.

Once a potential rule is identified, further evaluation is needed to determine whether it can be added as a formal rule into the existing network. In practice, only if the accuracy improvement (loss decrease) brought by this potential rule exceeds a certain threshold (see (18)), the formal network will increase with a new rule.

$$L_{hr} - L_g \geq T_g \quad (18)$$

where T_g is the threshold for adding a new rule, and L_{hr}

Algorithm 2: Rule growing step

Input : $\tilde{x}, \tilde{y}, B^C$
Procedure:
1 $N_g = \text{Size}(B^C)$;
2 **for** $h = 1$ to N_g **do**
3 Pre-generate a new hypothetical rule R_h ;
4 Randomly initialize the consequent parameters $c_j^{i,k}, s_j^{i,k}$ of R_h ;
5 Initialize the weight parameters of R_h as $q_i^k = q_r^k = q_o^k = 0.5$;
6 Initialize R_h 's antecedent IT2MF and co-antecedent MF using using (16) - (17) ;
7 Fix antecedent parameters and optimize all other parameters over the network Net_h using SGD;
8 Compute the loss L_h of the whole training set;
9 Sort loss L , then find the minimum one L_g and its corresponding rule R_g , cluster C_g and Net Net_g .
Output : L_g, R_g, C_g, Net_g

Algorithm 3: Rule removing step

Input : $\tilde{x}, \tilde{y}, B^R, B^S$
Procedure:
1 $N_r = \text{Size}(B^C)$;
2 **for** $h = 1$ to N_r **do**
3 Remove the h -th hypothetical rule from B^R and denote the network composed of remaining rules as Net_h ;
4 Fix antecedent parameters and optimize other parameters of Net_h using SGD;
5 Use the Net_h to compute the loss L_h over the whole training set;
6 Sort loss L , then find the minimum one L_r and its corresponding rule R_r and cluster C_r and Net_r .
Output : L_r, R_r, C_r, Net_r

is the the loss value of the existing network. To ensure a smooth growth of rules, the initial value of T_g is typically set to a very large value. Here, it is configured as 1e10.

It should be noted that, in the rule growing process, we consider the impact of multiple model outputs when calculating the loss values. Additionally, the common parameters in Layer 2 are kept unchanged, while all individual parameters in other layers are optimised together.

2) *Rule Removing step:* Once the rules stop growing, the rule removing step is introduced to prune insignificant rules for a compact network structure. This is carried out by excluding rules from the current network in sequence

Algorithm 4: Global optimization

Input : $\tilde{x}, \tilde{y}, B^R$
Procedure:
1 Optimize all parameters of Net_{gl} together using SGD, i.e. (21) ;
2 Compute the loss L_{gl} of the whole training set;
Output : Net_{gl}

(each episode can remove at most one rule), under the condition that the removal of a rule will result in a negligible increase in the loss value. The actual process is depicted in Algorithm 3. Here, each rule in the current network becomes a hypothetical removing rule R_h . The remaining rules after excluding R_h then construct a new hypothetical network Net_h . Similar to the rule growing step, each hypothetical network is optimized under fixed antecedent parameters. The hypothetical rule corresponding to the network Net_h with the smallest loss L_r becomes the potential rule R_r to be removed.

Then, only if the loss increase caused by this potential rule pruning falls below a certain threshold (see (19)), it can be removed from the current network. Otherwise, the rule is considered important without removal and the algorithm moves on to Stage 2.

$$L_{hr} - L_r < T_r \quad (19)$$

Here, T_r is the threshold for removing an existing rule. Furthermore, to ensure that the algorithm does not get stuck in an endless loop, $T_r \leq T_g$ must hold.

C. Stage 2: Parameter Fine-tuning

In Stage 1, at most one rule is allowed to be added or removed per episode. When the number of rules changes, the network undergoes a local parameter optimization. However, if the rule number remains constant throughout an episode, the Stage 2 optimisation is initiated to fine-tune the existing parameters globally. The implementations of stage 2 are depicted in Algorithm 4. Differing from the Stage 1, all parameters here ($n \cdot 3 \cdot M + 2 \cdot K \cdot n + (n+1) \cdot 2 \cdot M \cdot K + 2 \cdot K + K + 1$) are optimized using SGD. For each model output, the loss function E can be represented as:

$$E = \frac{1}{2} \sum_{k=1}^K (y^k - y_a^k)^2 \quad (20)$$

where y_a^k is the actual value of the k -th output.

Then, the parameters can be updated by gradient descent:

$$V = V - \eta \frac{\partial E}{\partial V} \quad (21)$$

where η is the learning rate and V represents the model parameters, i.e., $c_j^{i,k}, s_j^{i,k}, m_{1,j}^i, m_{2,j}^i, \sigma_j^i, m_j^k, \sigma_j^k, q_i^k, q_r^k, q_o^k, l$. The derivatives of these variables with respect to the loss function can be found in Supplement II of the supplementary materials.

To summarise, the pre-stage is initially performed for data preparation, and the rule base is set as empty. Then, the fuzzy model structure evolves in Stage 1. Here, rule growing and rule removing steps are performed to construct the rule base and locally optimize parameters for efficiency. Subsequently, the Stage 2 (parameter fine-tuning) is performed to globally fine-tune parameters. The learning iterates between Stage 1 and Stage 2 until the rule structure stabilizes, at which the final SOIT2FNN-MO model is obtained. It is worth highlighting that even if there is no rule added or removed in stage 1, the optimization in Stage 2 may still give the new possibility for rule change in the next episode. Therefore, the final model structure is only confirmed when

the number of rules remains unchanged after one complete round of stage 2 and stage 1 in sequence.

IV. SIMULATION AND RESULTS

This section will present a comprehensive evaluation of the proposed approach on both simulated and real-world datasets. We will first compare SOIT2FNN-MO with other state-of-the-art approaches, demonstrating its superiority in the prediction accuracy and resilience to uncertainty. This is followed by a detailed analysis regarding the structural design and sensitivity testing (i.e. cluster numbers). The root mean square error (RMSE) and mean percentage error (MPE) are employed as the evaluation metrics. All simulations were conducted by MATLAB under Windows 10 operating system, Intel Core i7-1185G7 3.00GHz 32.0 GB.

A. Example 1 (Chaotic Time Series Prediction)

We first evaluate the performance of SOIT2FNN-MO on the Mackey–Glass chaotic time series. The time series was generated using the following delay differential equation (DDE):

$$\frac{dx(t)}{dt} = \frac{0.2x(t-\tau)}{1+x^{10}(t-\tau)} - 0.1x(t) \quad (22)$$

where $\tau \geq 17$. As depicted in [47], [48], the system response was chaotic time series. Here, the initial conditions were set as: $\tau = 30$ and $x(0) = 1.2$ according to [38], [49], [50].

A total of 1500 data points were generated from the interval $t \in [31, 1530]$ (see Fig. S3 in the supplementary document). Here, the first 1000 points were employed for training while the remaining 500 points were used for testing. We then took a 9-input and 3-output prediction problem, i.e. $[x(t-18), x(t-16), x(t-14), x(t-12), x(t-10), x(t-8), x(t-6), x(t-4), x(t-2); x(t), x(t+2), x(t+4)]$. The relevant parameters were set as: $T_g = T_r = 0.0025$, $\eta = 0.03$, $N_c = 5$, $l = 0.1$, $Episode_{max} = 100$. In addition, the number of iterations in the optimisation within rule growing/removing and parameter fine-tuning were set as 1000 and 3000, respectively. Moreover, the composite learning framework for interval type-2 fuzzy neural network (CLF-IT2NN) [25] and our previous work (CNN-LSTM) [11] were employed for comparisons. It should be noted that Beke and Kumbasar [25] listed a total of 12 types of CLF-IT2NN based on different rule antecedents and consequents. Here, we chose S-IVL to be consistent with our approach (i.e. Gaussian antecedent and TSK consequent). Additionally, to avoid the potential problem of vanished rule firing strength, we also added a transformation layer ($\log(\cdot)$) to CLF-IT2NN.

Apart from the noise-free conditions, we also evaluate the performance of these algorithms against different levels of noises in the data (i.e., adding Gaussian noise with STDs of 10% and 30%, respectively). Fig. 3 shows an illustration of the predicted and actual values (over the test dataset without noises) using SOIT2FNN, based on SW, PM and MO schemes, respectively. Moreover, Tables I - III present the performance comparisons on both clean and noisy time series, where the results are averages of the three-step predictions. A more detailed comparison of RMSE and MPE

TABLE I: Performance comparison on models trained with clean chaotic time series in Example 1

Data	CNN-LSTM [11]			CLF-IT2NN [25]			SOIT2FNN		
	SW	PM	MO	SW	PM	MO	SW	PM	MO
①	0.01	0.01	0.01	0.04	0.04	0.04	0.06	0.04	0.03
②	0.90	0.86	0.72	4.89	3.13	3.30	5.41	3.45	2.71
③	0.01	0.01	0.01	0.04	0.04	0.04	0.06	0.04	0.03
④	0.92	0.88	0.77	3.80	3.71	3.77	5.67	3.69	3.16
⑤	0.15	0.15	0.15	0.20	0.17	0.17	0.19	0.18	0.17
⑥	16.2	15.9	16.2	21.4	19.1	19.0	19.9	18.8	18.6
⑦	0.39	0.39	0.39	0.62	0.53	0.53	0.81	0.49	0.50
⑧	77.4	75.0	74.9	70.3	68.3	68.4	86.9	67.5	67.2
Rule	—	—	—	2	2,2,2	2	1	1,2,2	2

Note: ①: Training RMSE (Clean); ②: Training MPE (Clean); ③: Test RMSE (Clean); ④: Test MPE (Clean); ⑤: Test RMSE (std=10%); ⑥: Test MPE (std=10%); ⑦: Test RMSE (std=30%); ⑧: Test MPE (std=30%). These also apply to Tables II - VII.

TABLE II: Performance comparison on models trained with noisy chaotic time series (std = 10%) in Example 1

Data	CNN-LSTM [11]			CLF-IT2NN [25]			SOIT2FNN		
	SW	PM	MO	SW	PM	MO	SW	PM	MO
⑨	0.14	0.12	0.12	0.13	0.13	0.13	0.13	0.13	0.13
⑩	14.5	14.4	14.2	15.0	14.0	15.2	14.9	14.7	14.8
③	0.06	0.05	0.05	0.06	0.06	0.05	0.05	0.05	0.05
④	5.68	5.00	5.12	5.55	5.22	5.22	5.39	5.09	4.90
⑤	0.14	0.14	0.14	0.19	0.17	0.15	0.14	0.14	0.14
⑥	14.6	15.9	15.9	18.4	16.6	16.3	15.9	15.5	15.4
⑦	0.38	0.36	0.36	0.40	0.39	0.37	0.35	0.35	0.35
⑧	83.8	81.4	76.1	51.2	46.1	45.2	41.5	41.2	41.4
Rule	—	—	—	2	2,2,3	3	2	2,2,2	2

⑨: Training RMSE (std=10%); ⑩: Training MPE (std=10%);

for each time-step prediction (i.e., $y^1 - y^3$) was provided in Tables S1-S3 in the supplements.

It can be observed that the proposed SOIT2FNN-MO models generally performed better than CLF-IT2FNN (both in RMSE and MPE), especially for the noisy data. Despite that CNN-LSTM achieved better results than SOIT2FNN-MO on the clean dataset, its performance rapidly declined with the increase of noise in the training data. In particular, our approach far outperformed CNN-LSTM when getting added noises with $std = 30\%$, demonstrating exceptional resilience to data uncertainty. When training models with noisy data (i.e., $std = 10\%$ and $std = 30\%$), the test performance of CNN-LSTM dropped to an unacceptable degree. Another interesting finding concerns the three schemes for multi-step ahead predictions. MO and PM exhibited better resilience to noises compared with SW. This can be attributed to the cumulative error during the window sliding process [51] in SW. Although PM performed similarly to MO on clean and low-noise (10%) datasets, it became obviously worse than the latter when the noise increased to 30%.

B. Example 2 (Microgrid Monitoring)

Multi-step time series forecasting in a microgrid energy system presents an essential task for network monitoring and control. This can involve the prediction of electricity

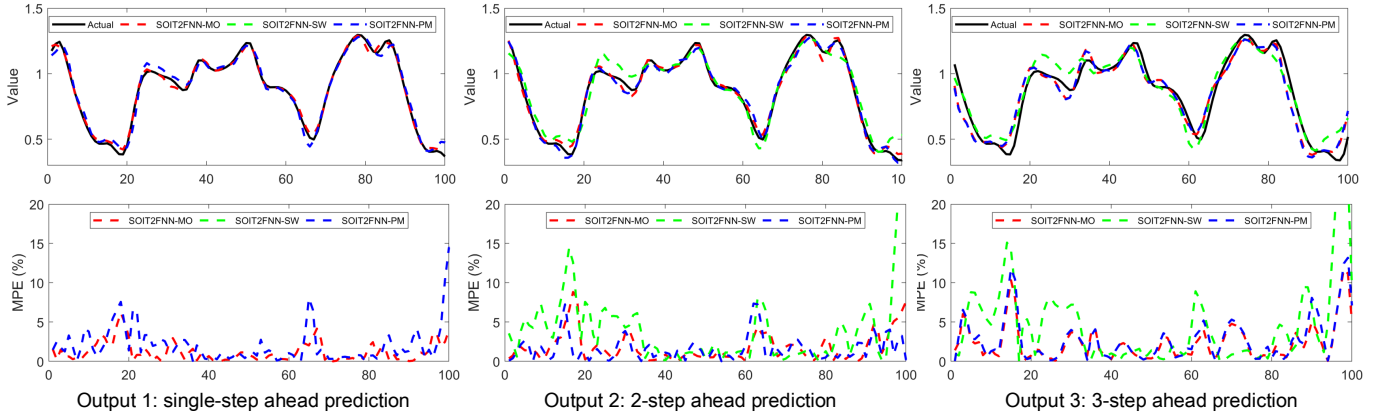


Fig. 3: A comparison of the prediction results on clean (test) chaotic time series in Example 1

TABLE III: Performance comparison on models trained with noisy chaotic time series (std=30%) in Example 1

Data	CNN-LSTM [11]			CLF-IT2NN [25]			SOIT2FNN		
	SW	PM	MO	SW	PM	MO	SW	PM	MO
①	0.11	0.07	0.11	0.37	0.40	0.36	0.36	0.42	0.34
②	16.3	9.27	16.3	30.0	30.4	26.3	29.7	34.9	25.9
③	0.34	0.31	0.32	0.19	0.21	0.18	0.17	0.24	0.16
④	32.8	31.4	32.1	18.9	19.7	16.7	21.5	22.8	15.7
⑤	0.38	0.34	0.34	0.26	0.23	0.19	0.21	0.27	0.19
⑥	38.4	36.6	35.1	26.3	23.5	23.0	27.4	27.1	22.0
⑦	0.64	0.59	0.56	0.41	0.44	0.39	0.36	0.41	0.36
⑧	115	102	96.1	57.2	59.3	48.6	55.0	46.2	44.5
Rule	—	—	—	3	2,3,3	5	2	2,3,3	5

①: Training RMSE (std=30%); ②: Training MPE (std=30%);

price and import/export energy (i.e. unmet power due to the lack/surplus of on-site renewable supplies) to meet the energy demand of a locality at the lowest cost. In this example, we evaluate the proposed SOIT2FNN-MO model on a real-world time series dataset [52], [53] collected from a US district microgrid system. This dataset contains unmet power and electricity price at a hourly resolution over a year. Here, to cover the seasonality effect, sensor measurements from the first 21 days of each month were extracted to form the training set, while the remaining data was used as test set. As a result, there are 6048 points in the training set and 2736 points in the test set. Illustrations of training and test sets were shown in Fig. S4 in the supplementary document.

We here used the time series of the past nine time steps (hours) to predict the values at the next three time steps. Unlike an autoregressive prediction (i.e., Chaotic time series prediction), we added three more variables to the model inputs to improve prediction accuracy and stability. Specifically, the time features (i.e., month, weekday and hour) of the nearest time step of each time series were used. Thus, the proposed SOIT2FNN-MO model has 12 inputs and 3 outputs, denoted as: $[m(t-1), w(t-1), h(t-1), v(t-9), v(t-8), v(t-7), v(t-6), v(t-5), v(t-4), v(t-3), v(t-2), v(t-1); v(t), v(t+1), v(t+2)]$. Here, $v(t)$ is the unmet power or electricity price at time instant t , while $m(t-1) \in [1, 12]$, $w(t-1) \in [1, 7]$, $h(t-1) \in [0, 23]$ are the month, weekday

TABLE IV: Performance comparison regarding RMSE and MPE on microgrid unmet power in Example 2

Data	CNN-LSTM [11]			CLF-IT2NN [25]			SOIT2FNN		
	SW	PM	MO	SW	PM	MO	SW	PM	MO
①	0.07	0.06	0.05	0.11	0.10	0.10	0.09	0.09	0.08
②	6.08	5.01	4.22	8.20	8.15	7.95	8.20	8.12	7.36
③	0.07	0.07	0.07	0.11	0.09	0.09	0.09	0.09	0.08
④	6.37	5.83	6.01	8.36	8.08	8.15	8.21	8.10	7.26
⑤	0.15	0.16	0.16	0.16	0.15	0.12	0.12	0.12	0.12
⑥	14.7	15.1	15.4	14.8	13.3	12.1	11.8	11.8	11.4
⑦	0.33	0.33	0.32	0.28	0.27	0.26	0.25	0.25	0.25
⑧	34.9	34.3	34.6	31.4	27.9	28.3	26.5	26.6	26.3
Rule	—	—	—	1	1,1,2	3	1	1,1,1	3

TABLE V: Performance comparison regarding RMSE and MPE on the electricity price in Example 2

Data	CNN-LSTM [11]			CLF-IT2NN [25]			SOIT2FNN		
	SW	PM	MO	SW	PM	MO	SW	PM	MO
①	0.06	0.05	0.05	0.09	0.08	0.08	0.08	0.8	0.07
②	9.09	8.13	8.28	12.8	11.9	12.3	11.5	11.3	10.9
③	0.06	0.06	0.06	0.08	0.08	0.08	0.07	0.07	0.07
④	10.2	9.26	9.75	12.0	11.7	11.7	11.7	11.5	11.2
⑤	0.09	0.09	0.09	0.12	0.10	0.10	0.09	0.09	0.09
⑥	15.8	15.9	16.2	20.0	18.4	17.6	17.1	16.5	16.4
⑦	0.18	0.19	0.21	0.19	0.17	0.17	0.16	0.16	0.16
⑧	40.6	44.8	48.1	42.5	37.9	38.3	37.9	37.2	36.7
Rule	—	—	—	1	1,1,2	3	1	1,1,1	2

and hour features at time instant $t-1$. Similar as in Example 1, Gaussian noises with variances of 10% and 30% were added to the dataset to simulate data uncertainty within the microgrid system. These parameters were set in the model determination process: $N_c = 5$ for unmet power prediction, $N_c = 10$ for price prediction and $T_g = T_r = 0.001$ for both predictions. Other parameters remained the same as those used in the previous example.

Figs. 4 and 5 show the predicted and actual values for the unmet power and electricity price (from 00:00 25th Jan to 03:00 29th Jan). Tables IV and V present the performance comparisons on clean and noisy datasets. More details on

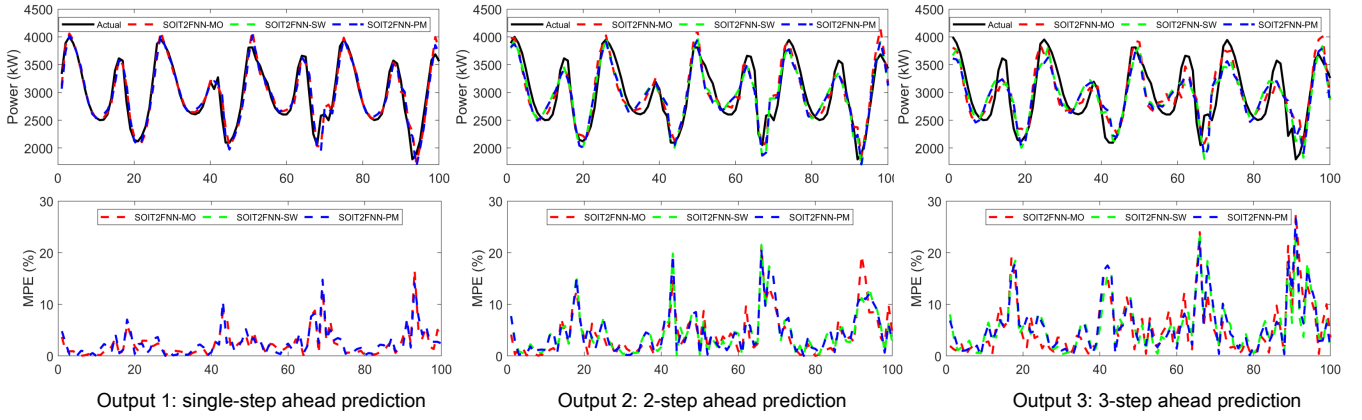


Fig. 4: Performance comparisons on unmet power in Example 2

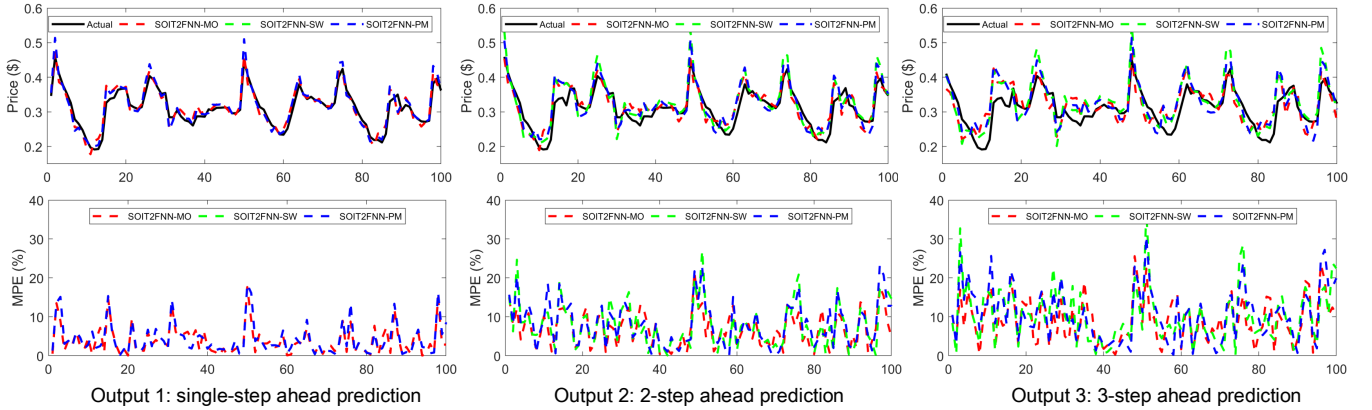


Fig. 5: Performance comparisons on electricity price in Example 2

each time step predictions were listed in Tables S4 and S5 of the supplements. It is evident that SOIT2FNN-MO still outperformed CLF-IT2FNN in this real-world dataset, even in the presence of added noises. Compared to Chaotic time series, our approach demonstrated better resilience in this example. For instance, SOIT2FNN-MO significantly outperformed CNN-LSTM in unmet power prediction when noise level was set to $std = 10\%$. This occurred earlier compared to the chaotic time series prediction, where SOIT2FNN-MO outperformed CNN-LSTM only when the noise level reached $std = 30\%$.

On the other hand, compared to CLF-IT2FNN, our approach has better network compactness (less number of rules) on both chaotic time series and microgrid management problems. It is worth mentioning that the total number of rules generated by the MO scheme was less than (or equal to) that generated by PM, and was more than that from SW. This is because PM involves the optimization of multiple single-step prediction models, while MO focuses on optimizing a single multi-step prediction model. In contrast, SW only needs to train one single-step prediction model.

C. Sensitivity and Structure Evaluations

In this subsection, we first study how the model structure and performance vary with the initial setting on the number of clusters in FCM. Table VI lists the comparison

results against different cluster numbers based on the clean datasets (see Table S6 in the supplementary materials for more details). Here, we can observe that the impact of clustering initialization on model accuracy was minor. In fact, SOIT2FNN-MO fine-tunes the antecedent parameters in Stage 2 learning, helping alleviate the impact of clustering initialization. As for the model structure, increasing the number of clusters appeared to have negligible effect on chaotic and power prediction and have an irregular effect on price prediction. Overall, it would be a good choice to have fewer clusters in the pre-stage learning, as it can significantly reduce the computational costs without sacrificing the accuracy too much.

Moreover, the structural design of the proposed SOIT2FNN-MO is also compared with the traditional structure of an IT2FNN (SIT2FNN: simplified interval type-2 neural fuzzy network) [38]. We added a transformation layer for SIT2FNN again to avoid the potential problem of vanished rule firing strength. The idea is to show if the newly introduced/modified layers in this paper can contribute to the model improvement. The results are given in Table VII; more details can be found in Table S7 in the supplements. It is evident that the new Layer 4 and modified Layer 6 improved the prediction accuracy. The new Layer 9 also demonstrated a positive impact on accuracy as it enhances temporal connections among

TABLE VI: Performance comparison regarding RMSE and MPE on clean training/test datasets regarding different clustering numbers

Data	No.=5	No.=10	No.=15	No.=20	No.=25	No.=30
①:Chaotic	0.027	0.028	0.025	0.024	0.026	0.023
②:Chaotic	2.709	3.081	2.626	2.407	2.816	2.416
③:Chaotic	0.031	0.035	0.031	0.029	0.034	0.029
④:Chaotic	3.157	3.862	3.109	2.939	3.589	2.935
Rule	2	2	2	2	2	2
①:power	0.084	0.085	0.083	0.083	0.082	0.081
②:power	7.358	7.362	7.190	7.213	7.174	7.033
③:power	0.080	0.081	0.079	0.079	0.078	0.077
④:power	7.258	7.377	7.204	7.219	7.074	7.029
Rule	3	3	3	3	3	4
①:price	0.077	0.074	0.076	0.070	0.074	0.081
②:price	11.61	10.90	11.18	10.68	10.86	12.45
③:price	0.072	0.068	0.071	0.066	0.068	0.074
④:price	11.68	11.22	11.32	11.04	11.08	12.45
Rule	1	2	1	3	2	1

TABLE VII: Performance evaluation for each modified/added layer (models trained with clean data)

Data	SIT2FNN [38]	Our approach	SIT2FNN + La. 4	SIT2FNN + La. 6	SIT2FNN + La. 9
③:Chaotic	0.041	0.031	0.043	0.031	0.039
④:Chaotic	4.548	3.157	4.216	3.315	4.292
⑤:Chaotic	0.173	0.165	0.169	0.176	0.173
⑥:Chaotic	20.27	18.61	18.66	19.79	20.00
⑦:Chaotic	0.529	0.496	0.492	0.503	0.490
⑧:Chaotic	73.28	67.20	69.38	69.32	66.63
Rule	3	2	3	2	3
③:power	0.086	0.080	0.083	0.089	0.086
④:power	8.152	7.258	7.758	8.050	8.154
⑤:power	0.120	0.116	0.118	0.117	0.117
⑥:power	12.65	11.38	12.54	11.58	11.69
⑦:power	0.265	0.249	0.253	0.250	0.250
⑧:power	28.26	26.27	26.19	25.65	25.87
Rule	2	3	3	1	2
③:price	0.083	0.068	0.073	0.074	0.073
④:price	12.79	11.22	11.79	11.49	11.36
⑤:price	0.092	0.086	0.088	0.088	0.088
⑥:price	17.47	16.43	16.43	17.73	16.08
⑦:price	0.169	0.160	0.164	0.161	0.160
⑧:price	36.83	36.67	36.74	38.43	36.96
Rule	2	2	2	2	2

La.: Layer

multi-step predictions. Overall, the proposed SOIT2FNN-MO incorporating all these three layers achieved the best performance for multi-step time series predictions.

D. Interpretability Evaluation

Finally, the interpretability of the proposed SOTT2FNN-MO model is also evaluated using the chaotic time series data. As shown in Table I, SOIT2FNN resulted in a 2-rule network. We visualize the firing strength of each rule on all 500 test samples, as shown in Fig. 6 (a) and (b). Here, $F^{i,k}$ (i.e., firing strength of the i -th rule with respect to the k -th

output/prediction, as shown in (6)) is the output of Layer 5 and F^i (if there is no Layer 4, i.e., traditional IT2FNN) is defined as:

$$F^i = [\underline{f}^i, \bar{f}^i], \quad i = 1, \dots, M \quad (23)$$

where the lower bound (\underline{f}^i) and upper bound (\bar{f}^i) of F^i can be expressed as:

$$\begin{aligned} \underline{f}^i &= -\frac{1}{\log(\underline{R}^i)} = -\frac{1}{\sum_{j=1}^n \log(\underline{\mu}_j^i(x_j))} \\ &= -\frac{1}{\sum_{j=1}^n \log(\underline{\mu}_j^i(x_j))} \end{aligned} \quad (24)$$

$$\begin{aligned} \bar{f}^i &= -\frac{1}{\log(\bar{R}^i)} = -\frac{1}{\sum_{j=1}^n \log(\bar{\mu}_j^i(x_j))} \\ &= -\frac{1}{\sum_{j=1}^n \log(\bar{\mu}_j^i(x_j))} \end{aligned} \quad (25)$$

It can be observed from the two figures (comparison between F^i and $F^{i,k}$) that the new co-antecedent layer (Layer 4) gave a more concentrated distribution of firing strength in both rules. In most cases, rule 1 may have a greater impact than rule 2 as the firing strength of the former is generally larger. For more details, we picked the 100th sample $\tilde{x} = [0.9810, 1.0408, 1.1740, 1.1630, 1.0770, 1.1085, 1.2025, 1.1471, 1.1177]$ as an example for further analysis. The corresponding firing strengths (F^i and $F^{i,k}$) of both rules are marked in Fig. 6 (a) and (b), respectively. We can find that the firing strength of rule 1 is much higher than that of rule 2. Moreover, the firing strengths for all three predictions are very close in both rules. This is because SOIT2FNN-MO is designed for multi-step time-series predictions, and there are clear temporal dependencies (very close values) among the three outputs. Unlike Layer 2 and Layer 3 (which work for all multi-step predictions), Layer 4 is an output-oriented layer (i.e., it only plays an important role in one of the model outputs). In this manner, the presence of Layer 4 allows for a better interpretation of each prediction in multi-step time-series forecasting. It should be noted that while Layer 4 may also affect the predictions at other time steps due to the presence of the final link layer in the network; such effect is typically minimal. This is because link values l is generally very small, as elaborated later.

We then analyse the modified consequent layer (Layer 6) by visualizing its outputs for each rule on all 500 test samples, as shown in Fig. 6 (c) and (d). Similar to the role of Layer 4, the modified Layer 6 can present the behaviours of the prediction at each time step. However, unlike the patterns showed in firing strength, the distributions of the three outputs are quite different on each rule. This can be attributed to the principles of TSK fuzzy models, in which the rule antecedent (IF part) is employed to partition the whole input space into several local fuzzy regions, while the rule consequent (THEN part) is used to describe the system behaviours in each local region [54]. For multi-step prediction problems where the inputs are also time series, the local fuzzy regions corresponding to the rule antecedents can be quite similar. However, the system behaviours may

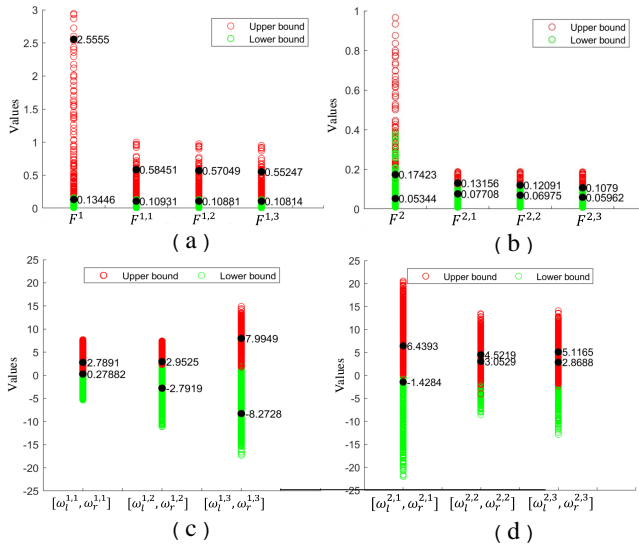


Fig. 6: The firing strengths of rule 1 (a) and rule 2 (b); the outputs of the modified consequent layer for rule 1 (c) and rule 2 (d)

generate different patterns depending on the design of the network structure.

In addition to the parameters in the rule antecedents and consequents mentioned above, other parameters also showed good interpretability. Specifically, the parameter q_o^k in Layer 8 indicates the importance of the interval boundaries y_l^k and y_r^k for the k -th prediction, while the link parameter l in Layer 9 demonstrates the significance between the prediction at the previous and current time steps for the final result. For chaotic time series prediction, we obtained the trained parameters as: $q_o^1 = 0.578$, $q_o^2 = 0.726$, $q_o^3 = 0.429$, $l = 0.124$. This suggests that the predictions at the first two steps are more likely to be influenced by the lower interval boundary. In contrast, the upper interval boundary influences the last prediction more. The predicted value from Layer 8 contributes to 87.6% of the final prediction, while the rest is attributed to predictions from previous time steps.

V. CONCLUSION

This paper proposed a new self-organizing interval type-2 fuzzy neural network based on a multi-output scheme (SOIT2FNN-MO) for multi-step time series prediction. The approach makes several key innovations to improve prediction accuracy, uncertainty handling and model interpretability. These include the development of a nine-layer deep network with a new co-antecedent layer for improving the interpretability of the rule antecedent, a transformation layer to address the problem of vanished rule firing strength for high-dimensional inputs, a modified consequent layer for improving interpretability of the rule consequent, and a new link layer to enhance temporal connections between multi-step ahead predictions. Furthermore, a two-stage self-organizing mechanism was developed to automatically generate rules and optimize all antecedent and consequent parameters. Extensive simulations were thereby conducted to confirm the effectiveness of the proposed approach in

terms of prediction accuracy, resilience to data uncertainty and model interpretability.

ACKNOWLEDGMENT

This work was supported in part by Royal Society and NSFC under grants IEC\NSFC\201107 and 62111530154.

REFERENCES

- [1] Shen, Y., Peng, Y., Shuai, Z., Zhou, Q., Zhu, L., Shen, Z. J., & Shahidepour, M. (2023). Hierarchical Time-Series Assessment and Control for Transient Stability Enhancement in Islanded Microgrids. *IEEE Transactions on Smart Grid*.
- [2] Zhang, Y., Shi, X., Zhang, S., & Abraham, A. (2022). A xgboost-based lane change prediction on time series data using feature engineering for autopilot vehicles. *IEEE Transactions on Intelligent Transportation Systems*, 23(10), 19187-19200.
- [3] Ray, P., Ganguli, B., & Chakrabarti, A. (2021). A hybrid approach of bayesian structural time series with lstm to identify the influence of news sentiment on short-term forecasting of stock price. *IEEE Transactions on Computational Social Systems*, 8(5), 1153-1162.
- [4] Lu, M., & Xu, X. (2024). TRNN: An efficient time-series recurrent neural network for stock price prediction. *Information Sciences*, 657, 119951.
- [5] Faisal, A. F., Rahman, A., Habib, M. T. M., Siddique, A. H., Hasan, M., & Khan, M. M. (2022). Neural networks based multi-variate time series forecasting of solar radiation using meteorological data of different cities of Bangladesh. *Results in Engineering*, 13, 100365.
- [6] Yuan, J., Wu, Y., Jing, W., Liu, J., Du, M., Wang, Y., & Liu, M. (2021). Association between meteorological factors and daily new cases of COVID-19 in 188 countries: A time series analysis. *Science of The Total Environment*, 780, 146538.
- [7] Moreno, J. E., Sanchez, M. A., Mendoza, O., Rodríguez-Díaz, A., Castillo, O., Melin, P., & Castro, J. R. (2020). Design of an interval Type-2 fuzzy model with justifiable uncertainty. *Information Sciences*, 513, 206-221.
- [8] Han, M., Zhong, K., Qiu, T., & Han, B. (2018). Interval type-2 fuzzy neural networks for chaotic time series prediction: A concise overview. *IEEE transactions on cybernetics*, 49(7), 2720-2731.
- [9] Sapankevych, N. I., & Sankar, R. (2009). Time series prediction using support vector machines: a survey. *IEEE computational intelligence magazine*, 4(2), 24-38.
- [10] Sagheer, A., & Kotb, M. (2019). Time series forecasting of petroleum production using deep LSTM recurrent networks. *Neurocomputing*, 323, 203-213.
- [11] Yao, F., Zhou, W., Al Ghamdi, M., Song, Y., & Zhao, W. (2022). An integrated D-CNN-LSTM approach for short-term heat demand prediction in district heating systems. *Energy Reports*, 8, 98-107.
- [12] Tang, Y., Yu, F., Pedrycz, W., Yang, X., Wang, J., & Liu, S. (2021). Building trend fuzzy granulation-based LSTM recurrent neural network for long-term time-series forecasting. *IEEE transactions on fuzzy systems*, 30(6), 1599-1613.
- [13] Mendel, J. M., & Wu, H. (2002, May). Uncertainty versus choice in rule-based fuzzy logic systems. In *2002 IEEE World Congress on Computational Intelligence. 2002 IEEE International Conference on Fuzzy Systems. FUZZ-IEEE'02. Proceedings (Cat. No. 02CH37291)* (Vol. 2, pp. 1336-1341). IEEE.
- [14] Pourabdollah, A., John, R., & Garibaldi, J. M. (2017, July). A new dynamic approach for non-singleton fuzzification in noisy time-series prediction. In *2017 IEEE International Conference on Fuzzy Systems (FUZZ-IEEE)* (pp. 1-6). IEEE.
- [15] Jafri, Y. Z., Waseem, A., Kamal, L., Raza, S. M., Sami, M., & Shah, S. H. (2012). Chaotic time series prediction and Mackey-Glass simulation with fuzzy logic. *Int J Phys Sci*, 7(17), 2596-2606.
- [16] Buckley, J. J., & Hayashi, Y. (1994). Fuzzy neural networks: A survey. *Fuzzy sets and systems*, 66(1), 1-13.
- [17] Jang, J. S. (1993). ANFIS: adaptive-network-based fuzzy inference system. *IEEE transactions on systems, man, and cybernetics*, 23(3), 665-685.
- [18] Melin, P., Soto, J., Castillo, O., & Soria, J. (2012). A new approach for time series prediction using ensembles of ANFIS models. *Expert Systems with Applications*, 39(3), 3494-3506.

- [19] Inyurt, S., & Razin, M. R. G. (2021). Regional application of ANFIS in ionosphere time series prediction at severe solar activity period. *Acta Astronautica*, 179, 450-461.
- [20] Khosravi, A., Nahavandi, S., Creighton, D., & Srinivasan, D. (2012). Interval type-2 fuzzy logic systems for load forecasting: A comparative study. *IEEE Transactions on Power Systems*, 27(3), 1274-1282.
- [21] Hisdal, E. (1981). The IF THEN ELSE statement and interval-valued fuzzy sets of higher type. *International Journal of Man-Machine Studies*, 15(4), 385-455.
- [22] Chen, C., & Vachtsevanos, G. (2012). Bearing condition prediction considering uncertainty: an interval type-2 fuzzy neural network approach. *Robotics and Computer-Integrated Manufacturing*, 28(4), 509-516.
- [23] Salimi-Badr, A. (2022). IT2CFNN: An interval type-2 correlation-aware fuzzy neural network to construct non-separable fuzzy rules with uncertain and adaptive shapes for nonlinear function approximation. *Applied Soft Computing*, 115, 108258.
- [24] Ashfahani, A., Pratama, M., Lughofer, E., Cai, Q., & Sheng, H. (2019). An online RFID localization in the manufacturing shopfloor. In *Predictive Maintenance in Dynamic Systems* (pp. 287-309). Springer, Cham.
- [25] Beke, A., & Kumbasar, T. (2022). More than accuracy: A composite learning framework for interval type-2 fuzzy logic systems. *IEEE Transactions on Fuzzy Systems*, 31(3), 734-744.
- [26] Luo, C., & Wang, H. (2020). Fuzzy forecasting for long-term time series based on time-variant fuzzy information granules. *Applied Soft Computing*, 88, 106046.
- [27] Mittal, K., Jain, A., Vaisla, K. S., Castillo, O., & Kacprzyk, J. (2020). A comprehensive review on type 2 fuzzy logic applications: Past, present and future. *Engineering Applications of Artificial Intelligence*, 95, 103916.
- [28] Chalapathy, R., Khoa, N. L. D., & Sethuvenkatraman, S. (2021). Comparing multi-step ahead building cooling load prediction using shallow machine learning and deep learning models. *Sustainable Energy, Grids and Networks*, 28, 100543.
- [29] Chandra, R., Goyal, S., & Gupta, R. (2021). Evaluation of deep learning models for multi-step ahead time series prediction. *IEEE Access*, 9, 83105-83123.
- [30] Taieb, S. B., Bontempi, G., Atiya, A. F., & Sorjamaa, A. (2012). A review and comparison of strategies for multi-step ahead time series forecasting based on the NN5 forecasting competition. *Expert systems with applications*, 39(8), 7067-7083.
- [31] Soto, J., Castillo, O., Melin, P., & Pedrycz, W. (2019). A new approach to multiple time series prediction using MIMO fuzzy aggregation models with modular neural networks. *International Journal of Fuzzy Systems*, 21, 1629-1648.
- [32] Han, H., Liu, Z., Liu, H., Qiao, J., & Chen, C. P. (2021). Type-2 fuzzy broad learning system. *IEEE Transactions on Cybernetics*, 52(10), 10352-10363.
- [33] Han, H., Sun, C., Wu, X., Yang, H., & Qiao, J. (2022). Self-organizing interval type-2 fuzzy neural network using information aggregation method. *IEEE Transactions on Neural Networks and Learning Systems*.
- [34] Han, H., Sun, C., Wu, X., Yang, H., & Qiao, J. (2022). Self-Organizing Interval Type-2 Fuzzy Neural Network with Adaptive Discriminative Strategy. *IEEE Transactions on Fuzzy Systems*.
- [35] Wang, P., Zhao, T., Cao, J., & Li, P. (2024). Soft Sensor Modeling of Self-Organizing Interval Type-2 Fuzzy Neural Network Based on Adaptive Quantum-Behaved Particle Swarm Optimization Algorithm. *International Journal of Fuzzy Systems*, 1-14.
- [36] Feng, L., Zhao, T., & Shang, Y. (2022, October). Soft sensor based on self-organizing interval type-2 fuzzy neural network and its application. In *7th International Symposium on Advances in Electrical, Electronics, and Computer Engineering* (Vol. 12294, pp. 483-490). SPIE.
- [37] Zhou, K., Oh, S. K., Qiu, J., Pedrycz, W., Seo, K., & Yoon, J. H. (2024). Design of Hierarchical Neural Networks Using Deep LSTM and Self-organizing Dynamical Fuzzy-Neural Network Architecture. *IEEE Transactions on Fuzzy Systems*.
- [38] Lin, Y. Y., Liao, S. H., Chang, J. Y., & Lin, C. T. (2013). Simplified interval type-2 fuzzy neural networks. *IEEE transactions on neural networks and learning systems*, 25(5), 959-969.
- [39] Luo, C., Tan, C., Wang, X., & Zheng, Y. (2019). An evolving recurrent interval type-2 intuitionistic fuzzy neural network for online learning and time series prediction. *Applied Soft Computing*, 78, 150-163.
- [40] Asadi, R., Yeganefar, A., & Niknam, S. A. (2019). Optimization and prediction of surface quality and cutting forces in the milling of aluminum alloys using ANFIS and interval type 2 neuro fuzzy network coupled with population-based meta-heuristic learning methods. *The International Journal of Advanced Manufacturing Technology*, 105, 2271-2287.
- [41] Taieb, S. B., Bontempi, G., Atiya, A. F., & Sorjamaa, A. (2012). A review and comparison of strategies for multi-step ahead time series forecasting based on the NN5 forecasting competition. *Expert systems with applications*, 39(8), 7067-7083.
- [42] Torshizi, A. D., Zarandi, M. H. F., & Zakeri, H. (2015). On type-reduction of type-2 fuzzy sets: A review. *Applied Soft Computing*, 27, 614-627.
- [43] Karnik, N. N., & Mendel, J. M. (2001). Centroid of a type-2 fuzzy set. *information SCIences*, 132(1-4), 195-220.
- [44] Juang, C. F., Huang, R. B., & Lin, Y. Y. (2009). A recurrent self-evolving interval type-2 fuzzy neural network for dynamic system processing. *IEEE Transactions on Fuzzy Systems*, 17(5), 1092-1105.
- [45] Chen, C. S., & Lin, W. C. (2011). Self-adaptive interval type-2 neural fuzzy network control for PMSM drives. *Expert Systems with Applications*, 38(12), 14679-14689.
- [46] Bezdek, J. C., Ehrlich, R., & Full, W. (1984). FCM: The fuzzy c-means clustering algorithm. *Computers & geosciences*, 10(2-3), 191-203.
- [47] Juang, C. F., & Tsao, Y. W. (2008). A self-evolving interval type-2 fuzzy neural network with online structure and parameter learning. *IEEE transactions on fuzzy systems*, 16(6), 1411-1424.
- [48] Tung, S. W., Quek, C., & Guan, C. (2013). eT2FIS: An evolving type-2 neural fuzzy inference system. *Information Sciences*, 220, 124-148.
- [49] Juang, C. F., Huang, R. B., & Cheng, W. Y. (2010). An interval type-2 fuzzy-neural network with support-vector regression for noisy regression problems. *IEEE Transactions on fuzzy systems*, 18(4), 686-699.
- [50] Juang, C. F., & Lin, C. T. (1998). An online self-constructing neural fuzzy inference network and its applications. *IEEE transactions on Fuzzy Systems*, 6(1), 12-32.
- [51] Dong, H., Guo, X., Reichgelt, H., & Hu, R. (2020). Predictive power of ARIMA models in forecasting equity returns: a sliding window method. *Journal of Asset Management*, 21(6), 549-566.
- [52] FLYao123. (2023, July). District microgrid dataset on Github, Retrieved Aug. 2023, from: <https://github.com/FLYao123/District-microgrid-dataset>
- [53] Yao, F., Zhao, W., Forshaw, M., & Song, Y. (2024). A Holistic Power Optimization Approach for Microgrid Control Based on Deep Reinforcement Learning. arXiv preprint arXiv:2403.01013.
- [54] Zhao, W., Li, K., & Irwin, G. W. (2012). A new gradient descent approach for local learning of fuzzy neural models. *IEEE Transactions on Fuzzy Systems*, 21(1), 30-44.

Supplementary Materials - A New Self-organizing Interval Type-2 Fuzzy Neural Network for Multi-Step Time Series Prediction

Fulong Yao*, Wanqing Zhao, Matthew Forshaw, Yang Song

Abstract—This is the supplementary document of the paper entitled “A New Self-organizing Interval Type-2 Fuzzy Neural Network for Multi-Step Time Series Prediction” submitted to *IEEE Transactions on Fuzzy Systems*. Section 1 presents the supplement on preliminaries, while Section 2 gives the supplement on derivations. Section 3 provides the supplement on simulations.

I. SUPPLEMENT ON PRELIMINARIES

A. Interval Type 2 Fuzzy Set

The concept of type-2 fuzzy sets (T2FS) was pioneered by Zadeh [S1] as an extension of an ordinary fuzzy set (type-1 fuzzy set (T1FS)) [S2]. Unlike the T1FS whose membership grade is crisp, the degrees of membership in the T2FS are themselves fuzzy, also referred as ‘fuzzy-fuzzy set’ [S3]. In this way, T2FS has the ability to deal with uncertain information that cannot be handled by a T1FS. However, T2FS-based systems exhibit computational complexity arising from the type 2 to type 1 reduction [S4]. Given this, interval T2FS (IT2FS) was developed to strike a balance between computational efficiency and uncertainty handling.

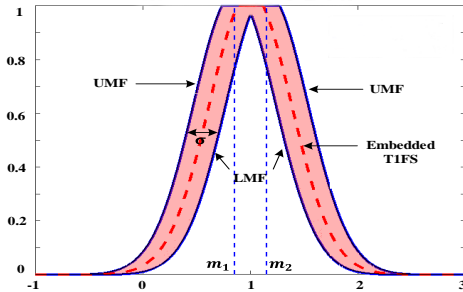


Fig. S1: An IT2FS with an uncertain mean, adapted from [S3]

The IT2FS is defined by an interval type 2 membership function (IT2MF) formed by an upper membership function (UMF) and a lower membership function (LMF). Fig. S1 illustrates an IT2FS with an uncertain mean. Here, data uncertainty is managed by representing membership values

Fulong Yao, Wanqing Zhao and Matthew Forshaw are with the School of Computing, Newcastle University, Newcastle Upon Tyne, NE4 5TG, UK. Yang Song is with the School of Mechanical and Electrical Engineering and Automation, Shanghai University, Shanghai, 200444, China. Corresponding author: Fulong Yao (F.Yao3@newcastle.ac.uk)

as intervals bound by the UMF and LMF [S5]. This interval, known as the footprint of uncertainty (FOU), captures the range of possible membership degrees for each element, thereby enabling IT2FS to robustly handle variations and uncertainties in data. Actually, T1FS is a special case of IT2FS. As showed in Fig. S1, the dashed line represents an embedded T1FS, while the solid lines form an IT2FS, illustrating how determinism is embedded within uncertainty [S3]. If the uncertainty (depicted by the pink shaded area) disappears, only the dashed line exists. In other words, once the corresponding intervals becomes a constant subset, randomness will degenerate into determinism, and IT2FS will also degenerate into T1FS. Therefore, IT2FS gives additional degrees of uncertainty in designing fuzzy logic systems (such as IT2FNN).

B. IT2FNN Model

Unlike traditional type-1 models, such as ANFIS, an IT2FNN model is made up of an IT2FS antecedent and an interval set (or crisp set) consequent. At present, the IT2FNN with a Gaussian MF and a TSK (Takagi-Sugeno-Kang) consequent exhibits superiority over its peer, serving as a standard choice in most applications [S6]. This can be expressed as a set of following IF-THEN rules:

$$\begin{aligned} \text{Rule } i : & \text{ IF } x_1 \text{ is } \tilde{A}_1^i \text{ AND... AND } x_n \text{ is } \tilde{A}_n^i \\ & \text{ THEN } w^{i,k} \text{ is } \tilde{a}_0^{i,k} + \sum_{j=1}^n \tilde{a}_j^{i,k} x_j \end{aligned} \quad (\text{S1})$$

where $x_1, \dots, x_j, \dots, x_n$ are model inputs, \tilde{A}_j^i is the IT2FS of the j -th input with regard to the i -th rule, $w^{i,k}$ is the k -th output of the i -th rule, and $\tilde{a}_j^{i,k} = [c_j^{i,k} - s_j^{i,k}, c_j^{i,k} + s_j^{i,k}]$ is an interval set. In this way, the uncertainty in data can be captured by both antecedent and consequent sets.

C. Multi-step Prediction Schemes

Multi-step prediction refers to the process of forecasting multiple future values in a time series. Unlike single-step prediction which forecasts the next immediate value, multi-step prediction aims to forecast several future points, thus providing a more comprehensive outlook on the future. At present, there are three popular schemes: sliding window (SW), paralleling model (PM) and multiple outputs (MO).

1) *Sliding window (SW)*: This scheme involves iteratively forecasting future time steps using previously predicted values, forming a sequential prediction process [30]. For example, Fig. S2 (a) shows the prediction process of the SW scheme for a 3-step ahead prediction problem using the past 6 values. Specifically, a 6-input single-output model is built to always make the prediction for the next time step, and then this predicted value is successively used to compose the input for predicting the value of the following time step. As this 6-1 window continues to slide, three predicted outputs are generated in sequence.

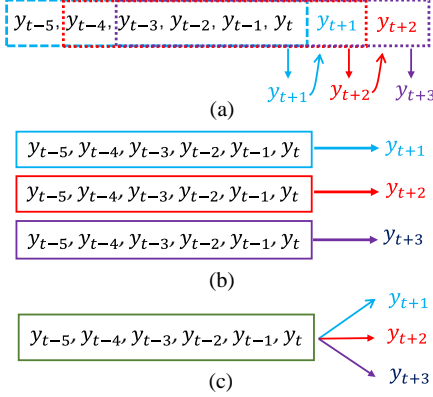


Fig. S2: Multi-step prediction schemes

2) *Paralleling model (PM)*: This scheme involves the development of separate models, each making a single prediction for a different future time step [30]. Fig. S2 (b) gives the prediction process of the PM scheme. Instead of just training a model for generating all future predictions, it needs to build each single-output model individually which is costly and time consuming.

3) *Multiple outputs (MO)*: This scheme uses a multi-output model to simultaneously predict multiple time series values into the future, without relying on the previous predictions [28]. Fig. S2 (c) illustrate the MO scheme. It trains a multi-output model capable of capturing complex temporal relationships across multiple time steps, providing all future predictions at one time.

REFERENCES

- [S1] Zadeh, L. A. (1975). The concept of a linguistic variable and its application to approximate reasoning—I. *Information sciences*, 8(3), 199-249.
- [S2] Zadeh, L. A. (1965). Fuzzy sets. *Information and control*, 8(3), 338-353.
- [S3] Mendel, J. M. (2007). Type-2 fuzzy sets and systems: an overview. *IEEE computational intelligence magazine*, 2(1), 20-29.
- [S4] Karnik, N. N., & Mendel, J. M. (1998, May). Introduction to type-2 fuzzy logic systems. In *1998 IEEE international conference on fuzzy systems proceedings. IEEE world congress on computational intelligence* (Cat. No. 98CH36228) (Vol. 2, pp. 915-920). IEEE.
- [S5] Liang, Q., & Mendel, J. M. (2000). Interval type-2 fuzzy logic systems: theory and design. *IEEE Transactions on Fuzzy systems*, 8(5), 535-550.
- [S6] Sun, C., Han, H., Wu, X., & Yang, H. (2023). Anti-Forgetting Incremental Learning Algorithm for Interval Type-2 Fuzzy Neural Network. *IEEE Transactions on Fuzzy Systems*.

II. SUPPLEMENT ON DERIVATIONS

A. Derivation of Gradients for (21)

The gradient derivations of the network parameters (i.e., $c_j^{i,k}$, $s_j^{i,k}$, $m_{1,j}^i$, $m_{2,j}^i$, σ_j^i , m_j^k , σ_j^k , q_l^k , q_r^k , q_o^k , l) can be expressed as follows:

$$\frac{\partial E}{\partial c_j^{i,k}} = \frac{\partial E}{\partial y^{k'}} \left(\frac{\partial y^{k'}}{\partial y_l^k} \frac{\partial y_l^k}{\partial w_l^{i,k}} \frac{\partial w_l^{i,k}}{\partial c_j^{i,k}} + \frac{\partial y^{k'}}{\partial y_r^k} \frac{\partial y_r^k}{\partial w_r^{i,k}} \frac{\partial w_r^{i,k}}{\partial c_j^{i,k}} \right) \quad (\text{S2})$$

$$\frac{\partial E}{\partial s_j^{i,k}} = \frac{\partial E}{\partial y^{k'}} \left(\frac{\partial y^{k'}}{\partial y_l^k} \frac{\partial y_l^k}{\partial w_l^{i,k}} \frac{\partial w_l^{i,k}}{\partial s_j^{i,k}} + \frac{\partial y^{k'}}{\partial y_r^k} \frac{\partial y_r^k}{\partial w_r^{i,k}} \frac{\partial w_r^{i,k}}{\partial s_j^{i,k}} \right) \quad (\text{S3})$$

$$\begin{aligned} \frac{\partial E}{\partial m_{1,j}^i} &= \sum_{k=1}^K \left[\frac{\partial E}{\partial y^{k'}} \left(\frac{\partial y^{k'}}{\partial y_l^k} \frac{\partial y_l^k}{\partial \bar{f}^{i,k}} + \frac{\partial y^{k'}}{\partial y_r^k} \frac{\partial y_r^k}{\partial \bar{f}^{i,k}} \right) \frac{\partial \bar{f}^{i,k}}{\partial m_{1,j}^i} \right] \\ &+ \sum_{k=1}^K \left[\frac{\partial E}{\partial y^{k'}} \left(\frac{\partial y^{k'}}{\partial y_l^k} \frac{\partial y_l^k}{\partial \underline{f}^{i,k}} + \frac{\partial y^{k'}}{\partial y_r^k} \frac{\partial y_r^k}{\partial \underline{f}^{i,k}} \right) \frac{\partial \underline{f}^{i,k}}{\partial m_{1,j}^i} \right] \end{aligned} \quad (\text{S4})$$

$$\begin{aligned} \frac{\partial E}{\partial m_{2,j}^i} &= \sum_{k=1}^K \left[\frac{\partial E}{\partial y^{k'}} \left(\frac{\partial y^{k'}}{\partial y_l^k} \frac{\partial y_l^k}{\partial \bar{f}^{i,k}} + \frac{\partial y^{k'}}{\partial y_r^k} \frac{\partial y_r^k}{\partial \bar{f}^{i,k}} \right) \frac{\partial \bar{f}^{i,k}}{\partial m_{2,j}^i} \right] \\ &+ \sum_{k=1}^K \left[\frac{\partial E}{\partial y^{k'}} \left(\frac{\partial y^{k'}}{\partial y_l^k} \frac{\partial y_l^k}{\partial \underline{f}^{i,k}} + \frac{\partial y^{k'}}{\partial y_r^k} \frac{\partial y_r^k}{\partial \underline{f}^{i,k}} \right) \frac{\partial \underline{f}^{i,k}}{\partial m_{2,j}^i} \right] \end{aligned} \quad (\text{S5})$$

$$\begin{aligned} \frac{\partial E}{\partial \sigma_j^i} &= \sum_{k=1}^K \left[\frac{\partial E}{\partial y^{k'}} \left(\frac{\partial y^{k'}}{\partial y_l^k} \frac{\partial y_l^k}{\partial \bar{f}^{i,k}} + \frac{\partial y^{k'}}{\partial y_r^k} \frac{\partial y_r^k}{\partial \bar{f}^{i,k}} \right) \frac{\partial \bar{f}^{i,k}}{\partial \sigma_j^i} \right] \\ &+ \sum_{k=1}^K \left[\frac{\partial E}{\partial y^{k'}} \left(\frac{\partial y^{k'}}{\partial y_l^k} \frac{\partial y_l^k}{\partial \underline{f}^{i,k}} + \frac{\partial y^{k'}}{\partial y_r^k} \frac{\partial y_r^k}{\partial \underline{f}^{i,k}} \right) \frac{\partial \underline{f}^{i,k}}{\partial \sigma_j^i} \right] \end{aligned} \quad (\text{S6})$$

$$\begin{aligned} \frac{\partial E}{\partial m_j^k} &= \sum_{i=1}^M \left[\frac{\partial E}{\partial y^{k'}} \left(\frac{\partial y^{k'}}{\partial y_l^k} \frac{\partial y_l^k}{\partial \bar{f}^{i,k}} + \frac{\partial y^{k'}}{\partial y_r^k} \frac{\partial y_r^k}{\partial \bar{f}^{i,k}} \right) \frac{\partial \bar{f}^{i,k}}{\partial m_j^k} \right] \\ &+ \sum_{i=1}^M \left[\frac{\partial E}{\partial y^{k'}} \left(\frac{\partial y^{k'}}{\partial y_l^k} \frac{\partial y_l^k}{\partial \underline{f}^{i,k}} + \frac{\partial y^{k'}}{\partial y_r^k} \frac{\partial y_r^k}{\partial \underline{f}^{i,k}} \right) \frac{\partial \underline{f}^{i,k}}{\partial m_j^k} \right] \end{aligned} \quad (\text{S7})$$

$$\begin{aligned} \frac{\partial E}{\partial \sigma_j^k} &= \sum_{i=1}^M \left[\frac{\partial E}{\partial y^{k'}} \left(\frac{\partial y^{k'}}{\partial y_l^k} \frac{\partial y_l^k}{\partial \bar{f}^{i,k}} + \frac{\partial y^{k'}}{\partial y_r^k} \frac{\partial y_r^k}{\partial \bar{f}^{i,k}} \right) \frac{\partial \bar{f}^{i,k}}{\partial \sigma_j^k} \right] \\ &+ \sum_{i=1}^M \left[\frac{\partial E}{\partial y^{k'}} \left(\frac{\partial y^{k'}}{\partial y_l^k} \frac{\partial y_l^k}{\partial \underline{f}^{i,k}} + \frac{\partial y^{k'}}{\partial y_r^k} \frac{\partial y_r^k}{\partial \underline{f}^{i,k}} \right) \frac{\partial \underline{f}^{i,k}}{\partial \sigma_j^k} \right] \end{aligned} \quad (\text{S8})$$

$$\frac{\partial E}{\partial q_l^k} = \frac{\partial E}{\partial y^{k'}} \frac{\partial y^{k'}}{\partial y_l^k} \frac{\partial y_l^k}{\partial q_l^k} \quad (\text{S9})$$

$$\frac{\partial E}{\partial q_r^k} = \frac{\partial E}{\partial y^{k'}} \frac{\partial y^{k'}}{\partial y_r^k} \frac{\partial y_r^k}{\partial q_r^k} \quad (\text{S10})$$

$$\frac{\partial E}{\partial q_o^k} = \frac{\partial E}{\partial y^{k'}} \frac{\partial y^{k'}}{\partial q_o^k} \quad (\text{S11})$$

$$\frac{\partial E}{\partial l} = \sum_{k=1}^K \frac{\partial E}{\partial y^{k'}} \frac{\partial y^{k'}}{\partial l} \quad (\text{S12})$$

where

$$\frac{\partial E}{\partial y^{k'}} = \sum_{k=k}^K \left(\frac{\partial E}{\partial y^{k'}} \frac{\partial y^{k'}}{\partial y^{k'}} \right) \quad (\text{S13})$$

$$\frac{\partial E}{\partial y^{\mathbf{k}}} = y^{\mathbf{k}} - y_a^{\mathbf{k}} \quad (\text{S14})$$

$$\frac{\partial y^{\mathbf{k}}}{\partial y^{k'}} = l^{\mathbf{k}-k}(1-l) \quad (\text{see - Supplement II-B}) \quad (\text{S15})$$

and

$$\frac{\partial y^{k'}}{\partial y_l^k} = q_o^k \quad (\text{S16})$$

$$\frac{\partial y^{k'}}{\partial y_r^k} = (1 - q_o^k) \quad (\text{S17})$$

$$\frac{\partial y_l^k}{\partial w_l^{i,k}} \frac{\partial w_l^{i,k}}{\partial c_j^{i,k}} = \frac{(1 - q_l^k) \underline{f}^{i,k} + q_l^k \bar{f}^{i,k}}{\sum_{i=1}^M (\underline{f}^{i,k} + \bar{f}^{i,k})} x_j \quad (\text{S18})$$

$$\frac{\partial y_r^k}{\partial w_r^{i,k}} \frac{\partial w_r^{i,k}}{\partial c_j^{i,k}} = \frac{(1 - q_r^k) \underline{f}^{i,k} + q_r^k \bar{f}^{i,k}}{\sum_{i=1}^M (\underline{f}^{i,k} + \bar{f}^{i,k})} x_j \quad (\text{S19})$$

$$\frac{\partial y_l^k}{\partial w_l^{i,k}} \frac{\partial w_l^{i,k}}{\partial s_j^{i,k}} = - \frac{(1 - q_l^k) \underline{f}^{i,k} + q_l^k \bar{f}^{i,k}}{\sum_{i=1}^M (\underline{f}^{i,k} + \bar{f}^{i,k})} |x_j| \quad (\text{S20})$$

$$\frac{\partial y_r^k}{\partial w_r^{i,k}} \frac{\partial w_r^{i,k}}{\partial s_j^{i,k}} = \frac{(1 - q_r^k) \underline{f}^{i,k} + q_r^k \bar{f}^{i,k}}{\sum_{i=1}^M (\underline{f}^{i,k} + \bar{f}^{i,k})} |x_j| \quad (\text{S21})$$

$$\frac{\partial y_l^{k'}}{\partial y_l^k} \frac{\partial y_l^k}{\partial q_l^k} = \frac{\sum_{i=1}^M (\bar{f}^{i,k} - \underline{f}^{i,k}) w_l^{i,k}}{\sum_{i=1}^M (\underline{f}^{i,k} + \bar{f}^{i,k})} \quad (\text{S22})$$

$$\frac{\partial y_r^{k'}}{\partial y_r^k} \frac{\partial y_r^k}{\partial q_r^k} = \frac{\sum_{i=1}^M (\bar{f}^{i,k} - \underline{f}^{i,k}) w_r^{i,k}}{\sum_{i=1}^M (\underline{f}^{i,k} + \bar{f}^{i,k})} \quad (\text{S23})$$

$$\frac{\partial y^{k'}}{\partial q_o^k} = y_l^k - y_r^k \quad (\text{S24})$$

$$\frac{\partial y_l^k}{\partial \bar{f}^{i,k}} = \frac{q_l^k w_l^{i,k} - y_l^k}{\sum_{i=1}^M (\underline{f}^{i,k} + \bar{f}^{i,k})} \quad (\text{S25})$$

$$\frac{\partial y_r^k}{\partial \bar{f}^{i,k}} = \frac{q_r^k w_r^{i,k} - y_r^k}{\sum_{i=1}^M (\underline{f}^{i,k} + \bar{f}^{i,k})} \quad (\text{S26})$$

$$\frac{\partial y_l^k}{\partial \underline{f}^{i,k}} = \frac{(1 - q_l^k) w_l^{i,k} - y_l^k}{\sum_{i=1}^M (\underline{f}^{i,k} + \bar{f}^{i,k})} \quad (\text{S27})$$

$$\frac{\partial y_r^k}{\partial \underline{f}^{i,k}} = \frac{(1 - q_r^k) w_r^{i,k} - y_r^k}{\sum_{i=1}^M (\underline{f}^{i,k} + \bar{f}^{i,k})} \quad (\text{S28})$$

$$\frac{\partial y^{\mathbf{k}}}{\partial l} = \sum_{k=1}^{\mathbf{k}} (\mathbf{k} - k + 1) l^{\mathbf{k}-k} (y^{k-1'} - y^k) \quad (\text{see - Supplement II-B}) \quad (\text{S29})$$

$$\begin{aligned} \frac{\partial \bar{f}^{i,k}}{\partial m_{1,j}^i} &= \frac{\partial \bar{f}^{i,k}}{\partial \bar{R}^i} \frac{\partial \bar{R}^i}{\partial m_{1,j}^i} \\ &= \begin{cases} (\bar{f}^{i,k})^2 \times \frac{x_j - m_{1,j}^i}{(\sigma_j^i)^2}, & \text{if } x_j \leq m_{1,j}^i; \\ 0, & \text{otherwise.} \end{cases} \end{aligned} \quad (\text{S30})$$

$$\begin{aligned} \frac{\partial \underline{f}^{i,k}}{\partial m_{1,j}^i} &= \frac{\partial \underline{f}^{i,k}}{\partial \underline{R}^i} \frac{\partial \underline{R}^i}{\partial m_{1,j}^i} \\ &= \begin{cases} (\underline{f}^{i,k})^2 \times \frac{x_j - m_{1,j}^i}{(\sigma_j^i)^2}, & \text{if } x_j > \frac{m_{1,j}^i + m_{2,j}^i}{2}; \\ 0, & \text{otherwise.} \end{cases} \end{aligned} \quad (\text{S31})$$

$$\begin{aligned} \frac{\partial \bar{f}^{i,k}}{\partial m_{2,j}^i} &= \frac{\partial \bar{f}^{i,k}}{\partial \bar{R}^i} \frac{\partial \bar{R}^i}{\partial m_{2,j}^i} \\ &= \begin{cases} (\bar{f}^{i,k})^2 \times \frac{x_j - m_{2,j}^i}{(\sigma_j^i)^2}, & \text{if } x_j > m_{2,j}^i; \\ 0, & \text{otherwise.} \end{cases} \end{aligned} \quad (\text{S32})$$

$$\begin{aligned} \frac{\partial \underline{f}^{i,k}}{\partial m_{2,j}^i} &= \frac{\partial \underline{f}^{i,k}}{\partial \underline{R}^i} \frac{\partial \underline{R}^i}{\partial m_{2,j}^i} \\ &= \begin{cases} (\underline{f}^{i,k})^2 \times \frac{x_j - m_{2,j}^i}{(\sigma_j^i)^2}, & \text{if } x_j \leq \frac{m_{1,j}^i + m_{2,j}^i}{2}; \\ 0, & \text{otherwise.} \end{cases} \end{aligned} \quad (\text{S33})$$

$$\begin{aligned} \frac{\partial \bar{f}^{i,k}}{\partial \sigma_j^i} &= \frac{\partial \bar{f}^{i,k}}{\partial \bar{R}^i} \frac{\partial \bar{R}^i}{\partial \sigma_j^i} \\ &= \begin{cases} (\bar{f}^{i,k})^2 \times \frac{(x_j - m_{1,j}^i)^2}{(\sigma_j^i)^3}, & \text{if } x_j < m_{1,j}^i; \\ (\bar{f}^{i,k})^2 \times \frac{(x_j - m_{2,j}^i)^2}{(\sigma_j^i)^3}, & \text{if } x_j > m_{2,j}^i; \\ 0, & \text{otherwise.} \end{cases} \end{aligned} \quad (\text{S34})$$

$$\begin{aligned} \frac{\partial \underline{f}^{i,k}}{\partial \sigma_j^i} &= \frac{\partial \underline{f}^{i,k}}{\partial \underline{R}^i} \frac{\partial \underline{R}^i}{\partial \sigma_j^i} \\ &= \begin{cases} (\underline{f}^{i,k})^2 \times \frac{(x_j - m_{2,j}^i)^2}{(\sigma_j^i)^3}, & \text{if } x_j \leq \frac{m_{1,j}^i + m_{2,j}^i}{2}; \\ (\underline{f}^{i,k})^2 \times \frac{(x_j - m_{1,j}^i)^2}{(\sigma_j^i)^3}, & \text{if } x_j > \frac{m_{1,j}^i + m_{2,j}^i}{2}. \end{cases} \end{aligned} \quad (\text{S35})$$

$$\frac{\partial \bar{f}^{i,k}}{\partial m_j^k} = \frac{\partial \bar{f}^{i,k}}{\partial R^k} \frac{\partial R^k}{\partial m_j^k} = (\bar{f}^{i,k})^2 \times \frac{x_j - m_j^k}{(\sigma_j^k)^2} \quad (\text{S36})$$

$$\frac{\partial \underline{f}^{i,k}}{\partial m_j^k} = \frac{\partial \underline{f}^{i,k}}{\partial R^k} \frac{\partial R^k}{\partial m_j^k} = (\underline{f}^{i,k})^2 \times \frac{x_j - m_j^k}{(\sigma_j^k)^2} \quad (\text{S37})$$

$$\frac{\partial \bar{f}^{i,k}}{\partial \sigma_j^k} = \frac{\partial \bar{f}^{i,k}}{\partial R^k} \frac{\partial R^k}{\partial \sigma_j^k} = (\bar{f}^{i,k})^2 \times \frac{(x_j - m_j^k)^2}{(\sigma_j^k)^3} \quad (\text{S38})$$

$$\frac{\partial \underline{f}^{i,k}}{\partial \sigma_j^k} = \frac{\partial \underline{f}^{i,k}}{\partial R^k} \frac{\partial R^k}{\partial \sigma_j^k} = (\underline{f}^{i,k})^2 \times \frac{(x_j - m_j^k)^2}{(\sigma_j^k)^3} \quad (\text{S39})$$

The derivations of $\frac{\partial \bar{f}^{i,k}}{\partial m_{1,j}^i}$, $\frac{\partial \underline{f}^{i,k}}{\partial m_{1,j}^i}$, $\frac{\partial \bar{f}^{i,k}}{\partial m_{2,j}^i}$, $\frac{\partial \underline{f}^{i,k}}{\partial m_{2,j}^i}$, $\frac{\partial \bar{f}^{i,k}}{\partial \sigma_j^i}$, $\frac{\partial \underline{f}^{i,k}}{\partial \sigma_j^i}$, $\frac{\partial \bar{f}^{i,k}}{\partial m_j^k}$, $\frac{\partial \underline{f}^{i,k}}{\partial m_j^k}$, $\frac{\partial \bar{f}^{i,k}}{\partial \sigma_j^k}$ and $\frac{\partial \underline{f}^{i,k}}{\partial \sigma_j^k}$ can be found in Supplement II-C.

B. Derivation of $\frac{\partial y^{\mathbf{k}}}{\partial y^{k'}}$

Based on (15), the following can be derived:

$$\begin{aligned}
y^1 &= (1-l)y^{1'} + lx_n \\
y^2 &= (1-l)y^{2'} + ly^1 \\
&= (1-l)y^{2'} + l(1-l)y^{1'} + l^2x_n \\
y^3 &= (1-l)y^{3'} + ly^2 \\
&= (1-l)y^{3'} + l(1-l)y^{2'} + l^2(1-l)y^{1'} + l^3x_n \\
&\dots \\
y^k &= (1-l)y^{k'} + ly^k \\
&= (1-l)y^{k'} + \dots + l^{k-1}(1-l)y^{1'} + l^kx_n
\end{aligned} \tag{S40}$$

Then, it can be expressed explicitly as:

$$y^{\mathbf{k}} = \sum_{k=1}^{\mathbf{k}} l^{\mathbf{k}-k} (1-l)y^{k'} + l^{\mathbf{k}}x_n \tag{S41}$$

where $k, \mathbf{k} \in N^+$ and $k \leq \mathbf{k}$.

Therefore, the following holds:

$$\frac{\partial y^{\mathbf{k}}}{\partial y^{k'}} = l^{\mathbf{k}-k} (1-l) \tag{S42}$$

Further considering,

$$\begin{aligned}
\frac{\partial y^1}{\partial l} &= -y^{1'} + x_n \\
\frac{\partial y^2}{\partial l} &= -y^{2'} + y^{1'} - 2ly^{1'} + 2lx_n \\
\frac{\partial y^3}{\partial l} &= -y^{3'} + y^{2'} - 2ly^{2'} + 2ly^{1'} - 3l^2y^{1'} + 3l^2x_n \\
&\dots \\
\frac{\partial y^k}{\partial l} &= -y^{k'} + y^{k-1'} - \dots - kl^{k-1}y^{1'} + kl^{k-1}x_n
\end{aligned} \tag{S43}$$

and let $x_n = y^{0'}$, then the following can be obtained:

$$\frac{\partial y^{\mathbf{k}}}{\partial l} = \sum_{k=1}^{\mathbf{k}} (\mathbf{k} - k + 1) l^{\mathbf{k}-k} (y^{k-1'} - y^k) \tag{S44}$$

C. Derivation of $\frac{\partial \bar{f}^{i,k}}{\partial m_{1,j}^i}, \frac{\partial \underline{f}^{i,k}}{\partial m_{1,j}^i}, \frac{\partial \bar{f}^{i,k}}{\partial m_{2,j}^i}, \frac{\partial \underline{f}^{i,k}}{\partial m_{2,j}^i}, \frac{\partial \bar{f}^{i,k}}{\partial \sigma_j^i}, \frac{\partial \underline{f}^{i,k}}{\partial \sigma_j^i}, \frac{\partial \bar{f}^{i,k}}{\partial m_j^k}, \frac{\partial \underline{f}^{i,k}}{\partial m_j^k}, \frac{\partial \bar{f}^{i,k}}{\partial \sigma_j^k}, \frac{\partial \underline{f}^{i,k}}{\partial \sigma_j^k}$

According to (7) and (8), we have:

$$\frac{\partial \bar{f}^{i,k}}{\partial \bar{R}^i} = \frac{1}{\bar{R}^i R^k (\log(\bar{R}^i R^k))^2} R^k = \frac{(\bar{f}^{i,k})^2}{\bar{R}^i} \tag{S45}$$

$$\frac{\partial \underline{f}^{i,k}}{\partial \underline{R}^i} = \frac{1}{\underline{R}^i R^k (\log(\underline{R}^i R^k))^2} R^k = \frac{(\underline{f}^{i,k})^2}{\underline{R}^i} \tag{S46}$$

$$\frac{\partial \bar{f}^{i,k}}{\partial R^k} = \frac{1}{\bar{R}^i R^k (\log(\bar{R}^i R^k))^2} \bar{R}^i = \frac{(\bar{f}^{i,k})^2}{R^k} \tag{S47}$$

$$\frac{\partial \underline{f}^{i,k}}{\partial R^k} = \frac{1}{\underline{R}^i R^k (\log(\underline{R}^i R^k))^2} \underline{R}^i = \frac{(\underline{f}^{i,k})^2}{R^k} \tag{S48}$$

According to (1) - (5), these can be further derived:

$$\begin{aligned}
\frac{\partial \bar{R}^i}{\partial m_{1,j}^i} &= \frac{\partial \bar{R}^i}{\partial \bar{\mu}_j^i} \frac{\partial \bar{\mu}_j^i}{\partial m_{1,j}^i} \\
&= \begin{cases} \bar{R}^i \times \frac{x_j - m_{1,j}^i}{(\sigma_j^i)^2}, & \text{if } x_j \leq m_{1,j}^i; \\ 0, & \text{otherwise.} \end{cases}
\end{aligned} \tag{S49}$$

$$\begin{aligned}
\frac{\partial \underline{R}^i}{\partial m_{1,j}^i} &= \frac{\partial \underline{R}^i}{\partial \underline{\mu}_j^i} \frac{\partial \underline{\mu}_j^i}{\partial m_{1,j}^i} \\
&= \begin{cases} \underline{R}^i \times \frac{x_j - m_{1,j}^i}{(\sigma_j^i)^2}, & \text{if } x_j > \frac{m_{1,j}^i + m_{2,j}^i}{2}; \\ 0, & \text{otherwise.} \end{cases}
\end{aligned} \tag{S50}$$

$$\begin{aligned}
\frac{\partial \bar{R}^i}{\partial m_{2,j}^i} &= \frac{\partial \bar{R}^i}{\partial \bar{\mu}_j^i} \frac{\partial \bar{\mu}_j^i}{\partial m_{2,j}^i} \\
&= \begin{cases} \bar{R}^i \times \frac{x_j - m_{2,j}^i}{(\sigma_j^i)^2}, & \text{if } x_j > m_{2,j}^i; \\ 0, & \text{otherwise.} \end{cases}
\end{aligned} \tag{S51}$$

$$\begin{aligned}
\frac{\partial \underline{R}^i}{\partial m_{2,j}^i} &= \frac{\partial \underline{R}^i}{\partial \underline{\mu}_j^i} \frac{\partial \underline{\mu}_j^i}{\partial m_{2,j}^i} \\
&= \begin{cases} \underline{R}^i \times \frac{x_j - m_{2,j}^i}{(\sigma_j^i)^2}, & \text{if } x_j \leq \frac{m_{1,j}^i + m_{2,j}^i}{2}; \\ 0, & \text{otherwise.} \end{cases}
\end{aligned} \tag{S52}$$

$$\begin{aligned}
\frac{\partial \bar{R}^i}{\partial \sigma_j^i} &= \frac{\partial \bar{R}^i}{\partial \bar{\mu}_j^i} \frac{\partial \bar{\mu}_j^i}{\partial \sigma_j^i} \\
&= \begin{cases} \bar{R}^i \times \frac{(x_j - m_{1,j}^i)^2}{(\sigma_j^i)^3}, & \text{if } x_j < m_{1,j}^i; \\ \bar{R}^i \times \frac{(x_j - m_{2,j}^i)^2}{(\sigma_j^i)^3}, & \text{if } x_j > m_{2,j}^i; \\ 0, & \text{otherwise.} \end{cases}
\end{aligned} \tag{S53}$$

$$\begin{aligned}
\frac{\partial \underline{R}^i}{\partial \sigma_j^i} &= \frac{\partial \underline{R}^i}{\partial \underline{\mu}_j^i} \frac{\partial \underline{\mu}_j^i}{\partial \sigma_j^i} \\
&= \begin{cases} \underline{R}^i \times \frac{(x_j - m_{2,j}^i)^2}{(\sigma_j^i)^3}, & \text{if } x_j \leq \frac{m_{1,j}^i + m_{2,j}^i}{2}; \\ \underline{R}^i \times \frac{(x_j - m_{1,j}^i)^2}{(\sigma_j^i)^3}, & \text{if } x_j > \frac{m_{1,j}^i + m_{2,j}^i}{2}. \end{cases}
\end{aligned} \tag{S54}$$

$$\frac{\partial R^k}{\partial m_j^k} = \frac{\partial R^k}{\partial \mu_j^k} \frac{\partial \mu_j^k}{\partial m_j^k} = R^k \times \frac{x_j - m_j^k}{(\sigma_j^k)^2} \tag{S55}$$

$$\frac{\partial R^k}{\partial \sigma_j^k} = \frac{\partial R^k}{\partial \mu_j^k} \frac{\partial \mu_j^k}{\partial \sigma_j^k} = R^k \times \frac{(x_j - m_j^k)^2}{(\sigma_j^k)^3} \tag{S56}$$

Based on the above, finally the following quantities can be obtained:

$$\begin{aligned}
\frac{\partial \bar{f}^{i,k}}{\partial m_{1,j}^i} &= \frac{\partial \bar{f}^{i,k}}{\partial \bar{R}^i} \frac{\partial \bar{R}^i}{\partial m_{1,j}^i} \\
&= \begin{cases} (\bar{f}^{i,k})^2 \times \frac{x_j - m_{1,j}^i}{(\sigma_j^i)^2}, & \text{if } x_j \leq m_{1,j}^i; \\ 0, & \text{otherwise.} \end{cases}
\end{aligned} \tag{S57}$$

$$\begin{aligned}\frac{\partial \underline{f}^{i,k}}{\partial m_{1,j}^i} &= \frac{\partial \underline{f}^{i,k}}{\partial \underline{R}^i} \frac{\partial \underline{R}^i}{\partial m_{1,j}^i} \\ &= \begin{cases} (\underline{f}^{i,k})^2 \times \frac{x_j - m_{1,j}^i}{(\sigma_j^i)^2}, & \text{if } x_j > \frac{m_{1,j}^i + m_{2,j}^i}{2}; \\ 0, & \text{otherwise.} \end{cases}\end{aligned}\quad (\text{S58})$$

$$\begin{aligned}\frac{\partial \bar{f}^{i,k}}{\partial m_{2,j}^i} &= \frac{\partial \bar{f}^{i,k}}{\partial \bar{R}^i} \frac{\partial \bar{R}^i}{\partial m_{2,j}^i} \\ &= \begin{cases} (\bar{f}^{i,k})^2 \times \frac{x_j - m_{2,j}^i}{(\sigma_j^i)^2}, & \text{if } x_j > m_{2,j}^i; \\ 0, & \text{otherwise.} \end{cases}\end{aligned}\quad (\text{S59})$$

$$\begin{aligned}\frac{\partial \underline{f}^{i,k}}{\partial m_{2,j}^i} &= \frac{\partial \underline{f}^{i,k}}{\partial \underline{R}^i} \frac{\partial \underline{R}^i}{\partial m_{2,j}^i} \\ &= \begin{cases} (\underline{f}^{i,k})^2 \times \frac{x_j - m_{2,j}^i}{(\sigma_j^i)^2}, & \text{if } x_j \leq \frac{m_{1,j}^i + m_{2,j}^i}{2}; \\ 0, & \text{otherwise.} \end{cases}\end{aligned}\quad (\text{S60})$$

$$\begin{aligned}\frac{\partial \bar{f}^{i,k}}{\partial \sigma_j^i} &= \frac{\partial \bar{f}^{i,k}}{\partial \bar{R}^i} \frac{\partial \bar{R}^i}{\partial \sigma_j^i} \\ &= \begin{cases} (\bar{f}^{i,k})^2 \times \frac{(x_j - m_{1,j}^i)^2}{(\sigma_j^i)^3}, & \text{if } x_j < m_{1,j}^i; \\ (\bar{f}^{i,k})^2 \times \frac{(x_j - m_{2,j}^i)^2}{(\sigma_j^i)^3}, & \text{if } x_j > m_{2,j}^i; \\ 0, & \text{otherwise.} \end{cases}\end{aligned}\quad (\text{S61})$$

$$\begin{aligned}\frac{\partial \underline{f}^{i,k}}{\partial \sigma_j^i} &= \frac{\partial \underline{f}^{i,k}}{\partial \underline{R}^i} \frac{\partial \underline{R}^i}{\partial \sigma_j^i} \\ &= \begin{cases} (\underline{f}^{i,k})^2 \times \frac{(x_j - m_{2,j}^i)^2}{(\sigma_j^i)^3}, & \text{if } x_j \leq \frac{m_{1,j}^i + m_{2,j}^i}{2}; \\ (\underline{f}^{i,k})^2 \times \frac{(x_j - m_{1,j}^i)^2}{(\sigma_j^i)^3}, & \text{if } x_j > \frac{m_{1,j}^i + m_{2,j}^i}{2}. \end{cases}\end{aligned}\quad (\text{S62})$$

$$\frac{\partial \bar{f}^{i,k}}{\partial m_j^k} = \frac{\partial \bar{f}^{i,k}}{\partial R^k} \frac{\partial R^k}{\partial m_j^k} = (\bar{f}^{i,k})^2 \times \frac{x_j - m_j^k}{(\sigma_j^k)^2} \quad (\text{S63})$$

$$\frac{\partial \underline{f}^{i,k}}{\partial m_j^k} = \frac{\partial \underline{f}^{i,k}}{\partial R^k} \frac{\partial R^k}{\partial m_j^k} = (\underline{f}^{i,k})^2 \times \frac{x_j - m_j^k}{(\sigma_j^k)^2} \quad (\text{S64})$$

$$\frac{\partial \bar{f}^{i,k}}{\partial \sigma_j^k} = \frac{\partial \bar{f}^{i,k}}{\partial R^k} \frac{\partial R^k}{\partial \sigma_j^k} = (\bar{f}^{i,k})^2 \times \frac{(x_j - m_j^k)^2}{(\sigma_j^k)^3} \quad (\text{S65})$$

$$\frac{\partial \underline{f}^{i,k}}{\partial \sigma_j^k} = \frac{\partial \underline{f}^{i,k}}{\partial R^k} \frac{\partial R^k}{\partial \sigma_j^k} = (\underline{f}^{i,k})^2 \times \frac{(x_j - m_j^k)^2}{(\sigma_j^k)^3} \quad (\text{S66})$$

III. SUPPLEMENT ON SIMULATIONS

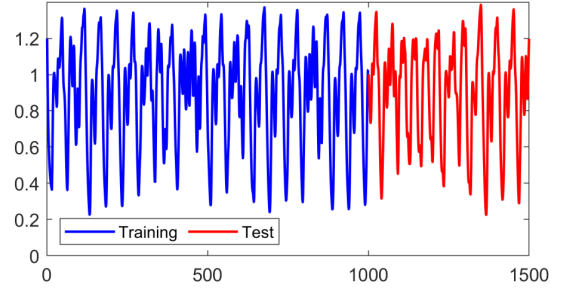


Fig. S3: An illustration of Chaotic time series in Example 1

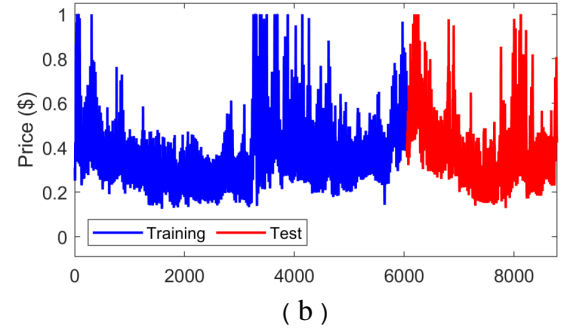
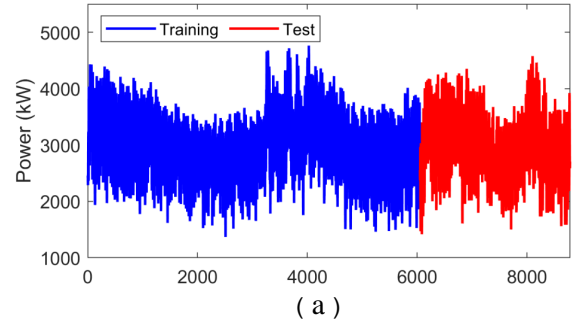


Fig. S4: Illustrations of the unmet power (a) and electricity price (b) in Example 2

TABLE S1: Performance comparison on models trained with clean chaotic time series in Example 1 (including results for each time step)

Data	CNN-LSTM [11]						CLF-IT2NN [25]						SOIT2FNN						SOIT2FNN-MO			
	SW		PM		MO		SW		PM		MO		SW		PM		SW		PM			
	y^1-y^3	Avg	y^1-y^3	Avg	y^1-y^3	Avg	y^1-y^3	Avg	y^1-y^3	Avg	y^1-y^3	Avg	y^1-y^3	Avg	y^1-y^3	Avg	y^1-y^3	Avg	y^1-y^3	Avg	y^1-y^3	Avg
Training	0.006	0.009	0.003	0.008	0.006	0.006	0.006	0.034	0.043	0.034	0.036	0.026	0.037	0.038	0.055	0.038	0.035	0.035	0.021	0.027		
RMSE (Clean)	0.009	0.007	0.014	0.006	0.007	0.006	0.044	0.030	0.030	0.030	0.038	0.038	0.061	0.030	0.030	0.030	0.027	0.027	0.027	0.027		
Training	0.603	0.903	0.319	0.858	0.605	0.722	3.315	4.892	3.115	3.132	2.189	3.298	3.612	5.413	3.612	3.446	2.196	2.709				
MPE (Clean)	0.941	0.709	1.546	0.887	0.887	4.921	2.925	2.925	2.925	2.932	2.932	6.016	3.049	3.049	3.049	2.886	3.046					
Test	0.006	0.009	0.003	0.008	0.006	0.007	0.035	0.043	0.035	0.039	0.032	0.040	0.038	0.057	0.038	0.036	0.024	0.031				
RMSE (Clean)	0.009	0.007	0.015	0.006	0.008	0.006	0.043	0.034	0.034	0.038	0.038	0.064	0.031	0.031	0.031	0.031	0.031	0.031	0.031	0.031		
Test	0.610	0.915	0.331	0.882	0.660	0.770	3.402	3.798	3.402	3.705	3.390	3.774	3.704	5.669	3.704	3.694	2.563	3.157				
MPE (Clean)	0.953	0.716	1.600	0.936	0.936	3.807	3.712	3.712	3.712	3.720	3.720	6.289	3.136	3.136	3.136	3.364	3.545					
Test	0.141	0.149	0.141	0.149	0.142	0.149	0.165	0.201	0.165	0.169	0.179	0.169	0.204	0.191	0.204	0.176	0.169	0.165				
RMSE (std=10%)	0.150	0.150	0.150	0.152	0.152	0.204	0.204	0.164	0.164	0.180	0.180	0.180	0.192	0.159	0.159	0.163	0.163	0.163	0.163	0.163		
Test	15.03	16.18	15.04	15.90	15.16	16.19	17.35	21.42	17.35	19.13	18.90	19.00	20.82	19.88	20.82	18.81	18.65	18.61				
MPE (std=10%)	16.39	16.05	16.60	16.50	16.50	22.94	17.01	17.01	17.01	20.13	20.13	20.01	17.24	17.24	17.24	18.73	18.73	18.61				
Test	0.371	0.390	0.368	0.392	0.369	0.390	0.499	0.621	0.499	0.534	0.545	0.527	0.641	0.805	0.641	0.491	0.561	0.496				
RMSE (std=30%)	0.393	0.399	0.410	0.392	0.392	0.593	0.572	0.572	0.572	0.502	0.502	0.816	0.417	0.510	0.417	0.510	0.416	0.496				
Test	69.17	77.44	69.01	75.04	70.10	74.88	64.31	70.25	64.31	68.32	72.25	68.39	84.36	86.90	84.36	67.46	79.00	67.20				
MPE (std=30%)	80.34	77.50	78.60	76.71	76.71	70.22	73.25	73.25	73.25	66.33	66.33	86.25	58.25	64.48	58.25	64.48	58.13	67.20				
Rule							2	2,2,2	2,2,2	2	2	1	1,2,2	2	1,2,2	2						

TABLE S2: Performance comparison on models trained with noisy chaotic time series (std = 10%) in Example 1 (including results for each time step)

Data	CNN-LSTM [11]						CLF-IT2NN [25]						SOIT2FNN						SOIT2FNN-MO					
	SW		PM		MO		SW		PM		MO		SW		PM		SW		PM		SW		PM	
	y^1-y^3	Avg	y^1-y^3	Avg	y^1-y^3	Avg	y^1-y^3	Avg	y^1-y^3	Avg	y^1-y^3	Avg	y^1-y^3	Avg	y^1-y^3	Avg	y^1-y^3	Avg	y^1-y^3	Avg	y^1-y^3	Avg	y^1-y^3	Avg
Training	0.129	0.137	0.121	0.124	0.119	0.122	0.123	0.134	0.123	0.131	0.128	0.133	0.127	0.128	0.125	0.128	0.125	0.128	0.125	0.125	0.125	0.125	0.125	0.130
RMSE	0.138		0.124		0.124		0.135		0.131		0.131		0.128		0.127		0.128		0.131		0.127		0.131	
(std=10%)	0.144		0.126		0.124		0.144		0.139		0.140		0.131		0.132		0.133		0.133		0.132		0.133	
Training	13.94	14.46	13.95	14.40	13.81	14.22	13.50	14.98	13.50	14.00	14.66	15.22	14.67	14.90	14.32	14.67	14.32	14.67	14.32	14.32	14.32	14.32	14.32	14.79
MPE	14.52		14.29		14.59		15.09		13.91		14.98		14.87		14.48		14.92		14.92		14.48		14.92	
(std=10%)	14.92		14.95		14.25		16.35		14.59		16.02		15.16		15.22		15.15		15.15		15.22		15.15	
Test	0.048	0.059	0.038	0.046	0.048	0.049	0.051	0.062	0.051	0.057	0.49	0.054	0.050	0.054	0.043	0.049	0.043	0.049	0.043	0.043	0.043	0.043	0.046	
RMSE	0.061		0.048		0.052		0.063		0.055		0.055		0.055		0.047		0.048		0.048		0.047		0.048	
(Clean)	0.068		0.052		0.047		0.072		0.065		0.058		0.057		0.058		0.048		0.048		0.058		0.048	
Test	4.737	5.683	4.122	4.998	4.805	5.119	5.136	5.547	5.136	5.216	4.887	5.219	5.048	5.385	4.555	5.085	4.555	5.085	4.555	4.555	4.555	4.555	4.901	
MPE	5.792		4.977		5.573		5.662		5.257		5.154		5.479		4.951		5.123		5.123		4.951		5.123	
(Clean)	6.520		5.894		4.980		5.843		5.255		5.616		5.626		5.748		5.027		5.027		5.748		5.027	
Test	0.133	0.142	0.131	0.140	0.135	0.140	0.157	0.191	0.157	0.173	0.140	0.152	0.134	0.142	0.131	0.139	0.131	0.139	0.131	0.131	0.131	0.131	0.140	
RMSE	0.143		0.141		0.142		0.188		0.180		0.151		0.144		0.139		0.141		0.141		0.139		0.141	
(std=10%)	0.150		0.148		0.145		0.228		0.182		0.165		0.148		0.148		0.148		0.148		0.148		0.148	
Test	13.70	14.59	14.62	15.91	15.16	15.92	15.62	18.39	15.62	16.55	15.02	16.32	14.76	15.92	14.35	15.51	14.35	15.51	14.35	14.35	14.35	14.35	15.40	
MPE	14.64		15.78		16.18		17.01		16.90		16.44		16.14		15.22		15.58		15.58		15.22		15.58	
(std=10%)	15.43		17.34		16.43		22.54		17.13		17.50		16.86		16.96		16.28		16.28		16.96		16.28	
Test	0.358	0.378	0.348	0.357	0.350	0.357	0.305	0.401	0.305	0.388	0.363	0.372	0.342	0.353	0.335	0.349	0.335	0.349	0.335	0.335	0.335	0.335	0.348	
RMSE	0.384		0.358		0.360		0.412		0.391		0.377		0.357		0.353		0.353		0.353		0.353		0.353	
(std=30%)	0.392		0.365		0.360		0.486		0.468		0.376		0.360		0.359		0.357		0.357		0.359		0.357	
Test	81.32	83.84	78.82	81.42	73.68	76.09	38.94	51.17	38.94	46.08	40.33	45.22	38.56	41.51	42.28	41.23	40.24	41.23	40.24	40.24	40.24	40.24	41.38	
MPE	82.68		79.84		77.35		52.24		45.51		47.87		41.34		40.11		41.61		41.61		40.11		41.61	
(std=30%)	87.52		85.59		77.23		62.33		53.79		47.46		44.64		41.29		42.28		42.28		41.29		42.28	
Rule							2		2,2,3		3		2		2,2,2		2		2,2,2		2		2	

TABLE S4: Performance comparison on microgrid unmet power in Example 2 (including results for each time step)

Data	CNN-LSTM [11]						CLF-IT2NN [25]						SOIT2FNN						SOIT2FNN-MO				
	SW		PM		MO		SW		PM		MO		SW		PM		SW		PM		Avg	$y^1 - y^3$	Avg
	$y^1 - y^3$	Avg	$y^1 - y^3$	Avg	$y^1 - y^3$	Avg	$y^1 - y^3$	Avg	$y^1 - y^3$	Avg	$y^1 - y^3$	Avg	$y^1 - y^3$	Avg	$y^1 - y^3$	Avg	$y^1 - y^3$	Avg	$y^1 - y^3$	Avg			
Training	0.044	0.070	0.044	0.061	0.037	0.052	0.082	0.111	0.075	0.097	0.079	0.103	0.057	0.091	0.057	0.090	0.054	0.084	0.084	0.084	0.084	0.084	0.084
RMSE	0.071		0.063		0.053		0.120		0.099		0.102		0.095		0.094		0.088		0.088		0.088		0.088
(Clean)	0.096		0.076		0.065		0.130		0.117		0.128		0.121		0.119		0.111		0.111		0.111		0.111
Training	3.308	6.083	3.212	5.013	2.943	4.215	6.403	8.203	7.882	8.154	6.210	7.945	4.668	8.198	4.668	8.116	4.291	7.358	7.358	7.358	7.358	7.358	7.358
MPE	6.110		5.203		4.245		7.615		8.165		7.825		8.520		8.445		7.610		7.610		7.610		7.610
(Clean)	8.831		6.624		5.457		10.59		8.415		9.801		11.40		11.23		10.17		10.17		10.17		10.17
Test	0.045	0.072	0.046	0.069	0.050	0.074	0.082	0.109	0.069	0.087	0.074	0.089	0.055	0.088	0.055	0.087	0.052	0.080	0.080	0.080	0.080	0.080	0.080
RMSE	0.073		0.072		0.077		0.099		0.092		0.088		0.091		0.090		0.084		0.084		0.084		0.084
(Clean)	0.098		0.091		0.095		0.146		0.100		0.105		0.117		0.115		0.105		0.105		0.105		0.105
Test	3.503	6.367	3.468	5.831	3.864	6.014	8.044	8.355	7.035	8.079	6.841	8.152	4.650	8.206	4.650	8.097	4.257	7.258	7.258	7.258	7.258	7.258	7.258
MPE	6.390		6.131		6.188		8.357		7.968		8.077		8.503		8.409		7.513		7.513		7.513		7.513
(Clean)	9.206		7.895		7.988		8.664		9.234		9.538		11.47		11.23		10.00		10.00		10.00		10.00
Test	0.114	0.152	0.107	0.155	0.109	0.157	0.129	0.162	0.110	0.145	0.093	0.123	0.095	0.120	0.095	0.120	0.093	0.116	0.116	0.116	0.116	0.116	0.116
RMSE	0.157		0.173		0.161		0.160		0.138		0.114		0.125		0.124		0.120		0.120		0.120		0.120
(std=10%)	0.186		0.187		0.200		0.197		0.187		0.162		0.140		0.140		0.136		0.136		0.136		0.136
Test	10.68	14.68	10.44	15.05	10.60	15.44	11.17	14.76	10.21	13.33	10.03	12.05	9.213	11.80	9.213	11.80	9.008	11.38	11.38	11.38	11.38	11.38	11.38
MPE	14.98		16.22		15.81		14.65		12.43		11.82		12.16		12.12		11.69		11.69		11.69		11.69
(std=10%)	18.38		18.49		19.92		18.46		17.35		14.30		14.02		14.05		13.44		13.44		13.44		13.44
Test	0.282	0.327	0.279	0.326	0.246	0.324	0.245	0.282	0.217	0.269	0.224	0.264	0.226	0.249	0.226	0.248	0.228	0.249	0.249	0.249	0.249	0.249	0.249
RMSE	0.328		0.346		0.328		0.288		0.263		0.259		0.253		0.251		0.252		0.252		0.252		0.252
(std=30%)	0.372		0.354		0.399		0.313		0.327		0.309		0.269		0.267		0.266		0.266		0.266		0.266
Test	28.98	34.88	28.99	34.34	26.76	34.56	25.34	31.42	22.57	27.88	24.48	28.31	24.12	26.48	24.12	26.60	23.75	26.27	26.27	26.27	26.27	26.27	26.27
MPE	34.79		35.98		34.58		29.09		28.10		26.83		26.93		27.09		26.78		26.78		26.78		26.78
(std=30%)	40.88		38.05		42.34		39.83		32.97		33.62		28.39		28.58		28.29		28.29		28.29		28.29
Rule							1		1,1,2		3		1		1,1,1		3		3		3		3

TABLE S5: Performance comparison on the electricity price in Example 2 (including results for each time step)

Data	CNN-LSTM [11]						CLF-IT2NN [25]						SOIT2FNN						SOIT2FNN-MO			
	SW		PM		MO		SW		PM		MO		SW		PM		SW		PM		Avg	Avg
	y^1-y^3	Avg	y^1-y^3	Avg	y^1-y^3	Avg	y^1-y^3	Avg	y^1-y^3	Avg	y^1-y^3	Avg	y^1-y^3	Avg	y^1-y^3	Avg	y^1-y^3	Avg	y^1-y^3	Avg		
Training	0.036	0.059	0.037	0.051	0.036	0.050	0.057	0.088	0.057	0.082	0.080	0.054	0.082	0.050	0.077	0.050	0.077	0.050	0.077	0.048	0.074	0.074
RMSE (Clean)	0.058		0.052		0.052		0.073		0.082		0.076		0.076		0.080		0.079		0.079	0.076		0.076
	0.081		0.063		0.064		0.134		0.101		0.116		0.101		0.101		0.101		0.101	0.096		0.096
Training	5.434	9.094	5.551	8.125	5.776	8.283	7.772	12.80	7.772	11.89	7.351	12.32	6.645	11.54	6.645	11.32	6.561	10.90	10.90			10.90
MPE (Clean)	9.103		8.342		8.604		11.56		10.98		11.25		11.81		11.59		11.26		11.26			11.26
	12.74		10.48		10.47		19.07		16.92		18.36		16.17		15.74		14.88		14.88			14.88
Test	0.039	0.061	0.038	0.056	0.040	0.058	0.052	0.080	0.052	0.078	0.049	0.076	0.045	0.072	0.045	0.071	0.044	0.068	0.068			0.068
RMSE (Clean)	0.062		0.058		0.060		0.092		0.081		0.073		0.074		0.074		0.071		0.071	0.071		0.071
	0.083		0.071		0.074		0.96		0.101		0.106		0.096		0.095		0.090		0.090			0.090
Test	5.942	10.18	5.806	9.256	6.431	9.748	6.983	12.00	6.983	11.71	7.021	11.73	6.582	11.73	6.582	11.47	6.497	11.22	11.22			11.22
MPE (Clean)	10.25		9.679		10.06		13.81		12.32		10.28		11.98		11.73		11.53		11.53			11.53
	14.34		12.28		12.75		15.21		15.83		17.89		16.62		16.11		15.63		15.63			15.63
Test	0.063	0.085	0.064	0.086	0.064	0.086	0.079	0.116	0.079	0.102	0.084	0.098	0.066	0.089	0.066	0.087	0.065	0.086	0.086			0.086
RMSE (std=10%)	0.086		0.086		0.087		0.099		0.095		0.098		0.091		0.089		0.088		0.088			0.088
	0.107		0.107		0.108		0.170		0.132		0.112		0.110		0.107		0.105		0.105			0.105
Test	12.16	15.82	12.37	15.85	12.42	16.19	12.73	20.02	12.73	18.44	15.35	17.56	12.78	17.09	12.78	16.47	12.60	16.43	16.43			16.43
MPE (std=10%)	15.70		15.72		16.21		19.97		18.34		17.42		17.24		16.56		16.61		16.61			16.61
	19.60		19.46		19.94		27.36		24.25		19.91		21.25		20.08		20.08		20.08			20.08
Test	0.159	0.175	0.160	0.193	0.164	0.205	0.135	0.189	0.135	0.172	0.140	0.173	0.149	0.163	0.149	0.160	0.146	0.160	0.160			0.160
RMSE (std=30%)	0.174		0.195		0.207		0.184		0.168		0.182		0.163		0.160		0.160		0.160			0.160
	0.193		0.224		0.246		0.248		0.213		0.197		0.178		0.172		0.175		0.175			0.175
Test	39.93	40.63	39.92	44.79	41.25	48.08	27.58	42.52	27.58	37.87	29.76	38.25	30.79	37.87	30.79	37.20	29.41	36.67	36.67			36.67
MPE (std=30%)	39.92		44.68		47.97		43.09		41.36		41.35		41.04		39.76		39.91		39.91			39.91
	42.05		49.77		55.03		56.89		44.67		43.64		41.79		41.04		40.69		40.69			40.69
Rule							1		1,1,2		3		1		1,1,1		2		2			2

TABLE S6: Performance comparison on clean training/test datasets regarding different clustering numbers (including results for each time step)

Data	No. = 5		No. = 10		No. = 15		No. = 20		No. = 25		No. = 30	
	$y^1 - y^3$	Avg	$y^1 - y^3$	Avg	$y^1 - y^3$	Avg	$y^1 - y^3$	Avg	$y^1 - y^3$	Avg	$y^1 - y^3$	Avg
Training	0.0213	0.0274	0.0224	0.0277	0.0192	0.0250	0.0198	0.0236	0.0204	0.0264	0.0203	0.0230
RMSE	0.0274		0.0306		0.0228		0.0228		0.0265		0.0224	
(Chaotic)	0.0334		0.0301		0.0329		0.0283		0.0322		0.0264	
Training	2.1962	2.7094	2.4307	3.0814	2.0508	2.6263	1.9870	2.4072	2.1455	2.8162	2.1010	2.4164
MPE	2.8857		3.4367		2.3792		2.3633		2.8160		2.3825	
(Chaotic)	3.0463		3.3767		3.4417		2.8712		3.4872		2.7656	
Test	0.0242	0.0305	0.0268	0.0346	0.0211	0.0307	0.0214	0.0293	0.0231	0.0342	0.0227	0.0286
RMSE	0.0312		0.0369		0.0299		0.0299		0.0354		0.0276	
(Chaotic)	0.0360		0.0402		0.0411		0.0367		0.0440		0.0356	
Test	2.5625	3.1571	2.9790	3.8622	2.2431	3.1090	2.2192	2.9386	2.4485	3.5890	2.3838	2.9345
MPE	3.3641		4.1745		2.8741		2.8950		3.6732		2.8115	
(Chaotic)	3.5446		4.4331		4.2097		3.7017		4.6452		3.6081	
Training	0.0544	0.0843	0.0544	0.0846	0.0531	0.0831	0.0533	0.0834	0.0535	0.0823	0.0281	0.0806
RMSE	0.0876		0.0879		0.0861		0.0864		0.0856		0.0700	
(power)	0.1109		0.1113		0.1100		0.1105		0.1079		0.1107	
Training	4.2908	7.3576	4.2961	7.3615	4.1641	7.1896	4.1779	7.2133	4.2301	7.1736	4.2122	7.0331
MPE	7.6103		7.6340		7.4007		7.4152		7.4380		7.2718	
(power)	10.172		10.154		10.004		10.047		9.8528		9.6151	
Test	0.0522	0.0803	0.0523	0.0810	0.0503	0.0787	0.0505	0.0790	0.0509	0.0783	0.0509	0.0774
RMSE	0.0837		0.0845		0.0817		0.0818		0.0812		0.0803	
(power)	0.1049		0.1062		0.1043		0.1047		0.1028		0.1011	
Test	4.2568	7.2580	4.3070	7.3772	4.1640	7.2036	4.1973	7.2185	4.1686	7.0742	4.2083	7.0293
MPE	7.5134		7.6535		7.4223		7.4204		7.3084		7.2520	
(power)	10.004		10.171		10.024		10.038		9.7455		9.6277	
Training	0.0499	0.0772	0.0484	0.0736	0.0495	0.0762	0.0469	0.0701	0.0484	0.0737	0.0524	0.0805
RMSE	0.0799		0.0762		0.0789		0.0725		0.0763		0.0826	
(price)	0.1018		0.0961		0.1002		0.0910		0.0965		0.1065	
Training	6.6753	11.606	6.5607	10.900	6.5872	11.178	6.5900	10.682	6.5521	10.8631	7.6863	12.453
MPE	11.849		11.257		11.509		11.047		11.1950		12.427	
(price)	16.294		14.882		15.444		14.407		14.8422		17.246	
Test	0.0455	0.0719	0.0439	0.0683	0.0200	0.0710	0.0436	0.0663	0.0438	0.0684	0.0480	0.0741
RMSE	0.0745		0.0707		0.0541		0.0687		0.0707		0.0761	
(price)	0.0958		0.0904		0.0892		0.0865		0.0907		0.0983	
Test	6.5861	11.680	6.4973	11.220	6.5114	11.320	6.6343	11.041	6.4226	11.084	7.6119	12.450
MPE	11.940		11.530		11.664		11.410		11.373		12.403	
(price)	16.574		15.634		15.784		15.079		15.455		17.335	
Rule (Chaotic)		2		2		2		2		2		2
Rule (power)		3		3		3		3		3		4
Rule (price)		1		2		1		3		2		1

TABLE S7: Performance evaluation for each modified/added layer (including results for each time step)

Data	SIT2FNN [38]		Our approach		SIT2FNN		SIT2FNN		SIT2FNN	
					with new layer 4		with modified layer 6		with new layer 9	
	y^1-y^3	Avg	y^1-y^3	Avg	y^1-y^3	Avg	y^1-y^3	Avg	y^1-y^3	Avg
Chaotic	0.040	0.041	0.024	0.031	0.037	0.043	0.024	0.031	0.033	0.039
Clean	0.040		0.031		0.045		0.031		0.042	
RMSE	0.043		0.040		0.046		0.039		0.042	
Chaotic	4.448	4.548	2.563	3.157	3.679	4.216	2.503	3.315	3.754	4.292
Clean	4.491		3.364		4.561		3.307		4.658	
MPE	4.706		3.545		4.407		4.136		4.464	
Chaotic	0.162	0.173	0.169	0.165	0.164	0.169	0.186	0.176	0.163	0.173
std=10%	0.174		0.163		0.165		0.167		0.175	
RMSE	0.181		0.164		0.179		0.176		0.182	
Chaotic	20.50	20.27	18.65	18.61	17.94	18.66	18.67	19.79	18.70	20.00
std=10%	19.73		18.73		18.26		20.03		19.98	
MPE	20.57		18.44		19.79		20.66		21.33	
Chaotic	0.578	0.529	0.561	0.496	0.474	0.492	0.520	0.503	0.491	0.490
std=30%	0.514		0.510		0.497		0.475		0.480	
RMSE	0.494		0.416		0.505		0.514		0.499	
Chaotic	73.79	73.28	79.00	67.20	64.87	69.38	80.21	69.32	68.84	66.63
std=30%	64.82		64.48		73.25		67.13		58.01	
MPE	81.22		58.13		70.02		60.62		73.03	
Power	0.057	0.086	0.052	0.080	0.054	0.083	0.057	0.089	0.057	0.086
Clean	0.087		0.084		0.087		0.092		0.087	
RMSE	0.113		0.105		0.109		0.117		0.113	
Power	5.158	8.152	4.257	7.258	4.556	7.758	4.584	8.050	5.137	8.154
Clean	8.339		7.513		8.188		8.313		8.336	
MPE	10.96		10.00		10.53		11.25		10.99	
Power	0.096	0.120	0.093	0.116	0.095	0.118	0.096	0.117	0.097	0.117
std=10%	0.125		0.120		0.120		0.119		0.119	
RMSE	0.140		0.136		0.138		0.137		0.136	
Power	10.10	12.65	9.008	11.38	10.20	12.54	9.386	11.58	9.560	11.69
std=10%	12.98		11.69		12.74		11.70		11.78	
MPE	14.88		13.44		14.67		13.67		13.72	
Power	0.255	0.265	0.228	0.249	0.240	0.253	0.232	0.250	0.242	0.250
std=30%	0.263		0.252		0.251		0.254		0.248	
RMSE	0.277		0.266		0.268		0.265		0.261	
Power	27.16	28.26	23.75	26.27	24.81	26.19	23.41	25.65	24.63	25.87
std=30%	27.95		26.78		26.22		26.28		25.90	
MPE	29.66		28.29		27.55		27.26		27.07	
Price	0.057	0.083	0.044	0.068	0.046	0.073	0.048	0.074	0.047	0.073
Clean	0.084		0.071		0.075		0.077		0.074	
RMSE	0.107		0.090		0.097		0.098		0.097	
Price	8.426	12.79	6.497	11.22	7.261	11.79	6.573	11.49	7.568	11.36
Clean	12.89		11.53		11.98		11.83		11.92	
MPE	17.06		15.63		16.13		16.07		16.10	
Price	0.068	0.092	0.065	0.086	0.065	0.088	0.066	0.088	0.065	0.088
std=10%	0.090		0.088		0.089		0.090		0.089	
RMSE	0.118		0.105		0.109		0.108		0.109	
Price	13.69	17.47	12.60	16.43	12.66	16.43	13.77	17.73	12.35	16.08
std=10%	18.70		16.61		16.55		17.96		16.18	
MPE	20.02		20.08		20.10		21.46		19.72	
Price	0.156	0.169	0.146	0.160	0.151	0.164	0.148	0.161	0.147	0.160
std=30%	0.168		0.160		0.163		0.162		0.159	
RMSE	0.184		0.175		0.179		0.174		0.175	
Price	29.09	36.83	29.41	36.67	29.14	36.74	31.50	38.43	29.25	36.96
std=30%	39.99		39.91		39.99		41.80		40.15	
MPE	41.40		40.69		41.10		41.98		41.47	
Rule (Chaotic)		3		2		3		2		3
Rule (power)		2		3		3		1		2
Rule (price)		2		2		2		2		2